POLITECNICO
MILANO 1863

SCUOLA DI INGEGNERIA INDUSTRIALE
E DELL'INFORMAZIONE

Mechanical Design of an RF Communications Prototype Puck to Validate Through-Ice Communications for Ocean World Technology Advancement

TESI DI LAUREA MAGISTRALE IN
MECHANICAL ENGINEERING-INGEGNERIA MECCANICA

Author: **Verónica Isabel Guerrero González**

Student ID:	10792504
Advisor:	Dr. Mario Guagliano
Co-advisor:	Dr. Bill Stone (Stone Aerospace, President & C.E.O.)
Academic Year:	2022-23

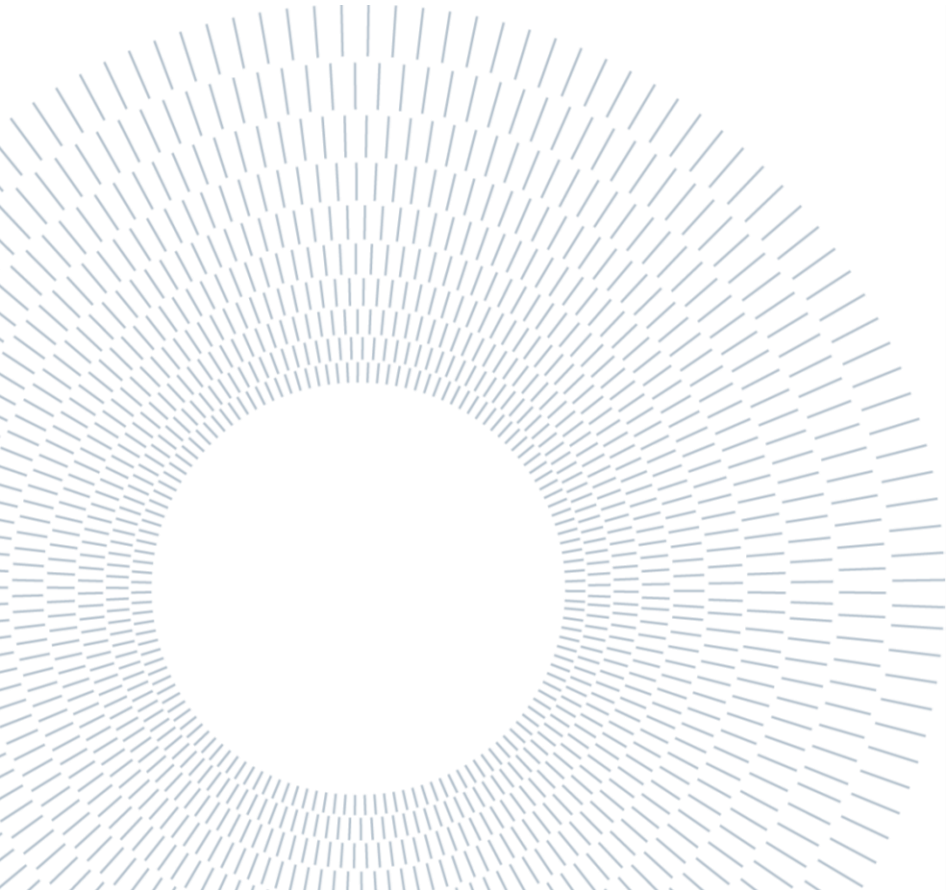

Abstract

Ocean Worlds are astronomical bodies—including moons, planets, and even comets—that harbor substantial liquid water, a fundamental ingredient for life as we know it. Several moons in our Solar System orbiting the outer planets have vast volumes of water beneath thick icy layers, making them prime candidates in the search for extraterrestrial life. Future missions to these moons envision landers deploying ice-penetrating vehicles, known as cryobots, to melt through the ice crust and explore the subglacial oceans. Among the engineering challenges, reliable communication technology is crucial for transmitting the valuable data collected by the cryobots back to Earth.

This study delves into the development of the PARTI Pucks Prototype, a specialized radio frequency (RF) communication solution intended for cryobot missions in Ocean Worlds and glacial environments. The prototype's development process is examined, focusing on critical aspects such as mechanical design, material selection, and thermal analysis. The prototype comprises several key components, including a patch antenna, crossed-loop antenna, electronics, and a water-resistant enclosure. Finite element analysis (FEA) was employed to validate the structural integrity of the housing and the FAM board. To optimize heat dissipation and evaluate the internal temperature profile, computational fluid dynamics (CFD) simulations were utilized for thermal behavior assessments within the prototype. Material trade-offs and configurations were meticulously explored throughout the development process, while ensuring that custom components were designed with manufacturability, assembly, and disassembly in mind. The prototype demonstrated satisfactory structural and thermal performance, underlining its potential as a noteworthy advancement in RF communication technology for cryobots. Moreover, this development process is presented as an invaluable case study that provides critical insights into design considerations and challenges. The study culminates by highlighting the lessons learned and the significant contributions of the prototype to both communication technology and mechanical design in remote environments.

Keywords: mechanical design, finite element analysis (FEA), computational fluid dynamics (CFD), product development, design for manufacturing, prototyping, radio frequency, Ocean World exploration.

Abstract in lingua italiana

I Mondi Oceanici sono corpi astronomici—compresi lune, pianeti e persino comete—che ospitano notevoli quantità di acqua allo stato liquido, un ingrediente fondamentale per la vita. Diverse lune nel nostro Sistema Solare contengono enormi volumi d'acqua al di sotto di spessi strati di ghiaccio, rendendole candidate di primo piano nella ricerca di vita extraterrestre. Le future missioni su queste lune prevedono l'invio di lander che dispieghino veicoli in grado di penetrare il ghiaccio, noti come cryobot, per fondere la crosta di ghiaccio ed esplorare gli oceani subglaciali. Tra le sfide ingegneristiche, una tecnologia di comunicazione affidabile è fondamentale per trasmettere alla Terra i preziosi dati raccolti dai cryobot.

Questo studio approfondisce lo sviluppo del Prototipo PARTI Pucks, una soluzione di comunicazione specializzata a radiofrequenza destinata a missioni con cryobot nei Mondi Oceanici e negli ambienti glaciali. Il prototipo comprende diversi componenti chiave, tra cui un'antenna patch, un'antenna a loop incrociato, l'elettronica e un involucro resistente all'acqua. L'analisi agli elementi finiti è stata impiegata per validare l'integrità strutturale dell'involucro e della scheda FAM. Per ottimizzare la dissipazione del calore, sono state utilizzate simulazioni di dinamica dei fluidi computazionale per valutare il comportamento termico all'interno del prototipo. I compromessi tra materiali e configurazioni sono stati esplorati durante il processo di sviluppo, garantendo al contempo che i componenti personalizzati fossero progettati tenendo presente la fabbricabilità, il montaggio e lo smontaggio. Il prototipo ha dimostrato prestazioni strutturali e termiche soddisfacenti, sottolineando il suo potenziale come progresso degno di nota nella tecnologia di comunicazione RF per cryobot. Inoltre, questo processo di sviluppo è presentato come uno studio di caso inestimabile che fornisce intuizioni critiche sulle considerazioni di progettazione e le sfide. Lo studio si conclude evidenziando le lezioni apprese e i significativi contributi del prototipo sia alla tecnologia di comunicazione che alla progettazione meccanica in ambienti remoti.

Parole chiave: progettazione meccanica, analisi agli elementi finiti (FEA), dinamica dei fluidi computazionale (CFD), sviluppo del prodotto, progettazione per la produzione, prototipazione, radiofrequenza, esplorazione dei Mondi Oceanici.

A mi familia, quien me enseñó a viajar
y a aprender de cada aventura.

Disclaimer

This Master's Thesis titled "Mechanical Design of an RF Communications Prototype Puck to Validate Through-Ice Communications for Ocean World Technology Advancement", submitted in partial fulfillment of the requirements for the degree of Master of Science in Mechanical Engineering at Politecnico di Milano, may contain certain proprietary information. This information is integral to the project and has been included with the express permission of the respective entities involved.

Any reproduction, distribution, publication, or use of any part of this thesis which includes the aforementioned proprietary information, in whole or in part, is strictly prohibited without the prior written authorization from the respective entity or entities holding the proprietary rights.

Individuals or organizations seeking to make use of any content that may involve proprietary information must contact the author and the respective entity to obtain written permission.

This disclaimer is intended to protect the intellectual property and proprietary rights of the involved entities, and to ensure that the content of this thesis is handled responsibly and ethically.

Please address all inquiries regarding proprietary information and permissions to:

Veronica Isabel Guerrero Gonzalez
veronica.guerrero@stoneaerospace.com

Stone Aerospace
admin@stoneaerospace.com

By accessing the contents of this thesis, you acknowledge that you have read, understood, and agreed to abide by the terms set forth in this proprietary information disclaimer.

Date: June 26th, 2023

Contents

Abstract ..... **iii**

Abstract in lingua italiana ..... **v**

Contents **1**

1 Introduction **3**

1.1 Context: Ocean World Exploration Technology 3

1.2 Aim and Scope of the Project 6

1.3 Prior Art 6

2 Requirements and Considerations **9**

2.1 Mission and Prototype Requirements 9

2.2 Design Considerations 11

2.2.1 High-Priority Design Considerations: 11

2.2.2 Medium-Priority Design Considerations: 12

2.2.3 Low-Priority Design Consideration: 12

2.2.4 Field Testing 12

3 Preliminary Design **15**

3.1 Patch Antenna 16

3.2 Crossed-Loop Antenna 17

3.3 Electronics 18

3.4 User Interface 18

3.5 Preliminary Design 19

4 Detailed Design **21**

4.1 Design for Manufacturing 22

4.1.1 Bill of Materials 22

4.1.2 Custom Components: Design and Material Selection 26
4.1.3 Fasteners: Material Selection 30
4.2 Design for Assembly and Disassembly 31
4.3 Component Highlights 35
4.3.1 Housing Manufacturing and Material Selection 35
4.3.2 O-ring Seal 37
4.3.3 EMI Enclosures 39
4.3.4 User Interface 41
4.4 Overall Costs 45
5 Analyses and Results 47
5.1 Structural Analyses 47
5.1.1 Housing 47
5.1.2 FAM Board 51
5.2 Thermal Analyses 55
5.2.1 Preliminary Thermal Analysis 56
5.2.2 Complete Thermal Analysis 57
6 Conclusions 64
Bibliography 66
A. Appendix A: EMI Shield Snap-Fit Design 69
B. Appendix B: Thermal Analysis Setup 77
I. List of Figures 83
II. List of Tables 87
III. List of Abbreviations 89
IV. List of Definitions 91
V. Acknowledgements 93

1 Introduction

1.1 Context: Ocean World Exploration Technology

Ocean Worlds are astronomical bodies that harbor substantial liquid water, a crucial ingredient for life as we know it. Several moons in our Solar System, orbiting the outer planets, contain vast volumes of water beneath thick icy layers, making them prime candidates for the discovery of microbial extraterrestrial life. To reach the subsurface ocean, a robotic vehicle must first traverse through kilometers of water ice. Communication through ice between a descending ice penetrating vehicle, or cryobot, and a surface lander is imperative for the successful retrieval of scientific data in subsurface missions on Ocean Worlds. Spooling out a high-bandwidth communication tether, such as a fiber optic cable, behind the cryobot as it descends, is considered both feasible and preferable as the primary means of communication [1,2]. However, due to the unpredictability of ice dynamics and the prolonged descent times of cryobots, ranging from several months to years, there is a substantial risk of the tether experiencing critical failures that could interrupt communications to the surface. Consequently, it is imperative for any deep ice exploration to incorporate a backup communication system with low bandwidth that does not depend on a tether. Addressing this need, Stone Aerospace [3], in partnership with the University of Colorado, and funded by the NASA COLDTech program, has initiated the PARTI-Pucks[1] project.

Figure 1: Concept of a Cryobot with an RF communications puck deployed for Ocean World exploration.

[1] PARTI-Pucks: **P**uck-based data transmission using **A**daptive **R**adio modems for **T**hrough-**I**ce communications.

This endeavor aims to design, manufacture, and conduct field tests on radio transceivers, often termed "pucks" by planetary science engineers, which could be strategically positioned behind a descending cryobot and embedded within the ice.

In the context of an ocean world mission, such as exploration on Jupiter's moon Europa, each puck is envisioned to function as a self-sustained relay, facilitating the transfer of messages through a series of discrete devices that are vertically deployed between the cryobot and the surface lander.

Stone Aerospace aims to advance ocean world through-ice communication technology that is long lived, low power, cold tolerant, and which addresses the environmental challenges posed by Europa, by designing and building radio frequency (RF) communication pucks with both ultra-high frequency (UHF) patch antennas and high frequency (HF) crossed-loop antennas to test and characterize their performance through 500 meters of terrestrial ice. A link test measuring data rate and signal strength through ice will advance the communications technology to TRL 5 and address elements of TRL 6 qualification.

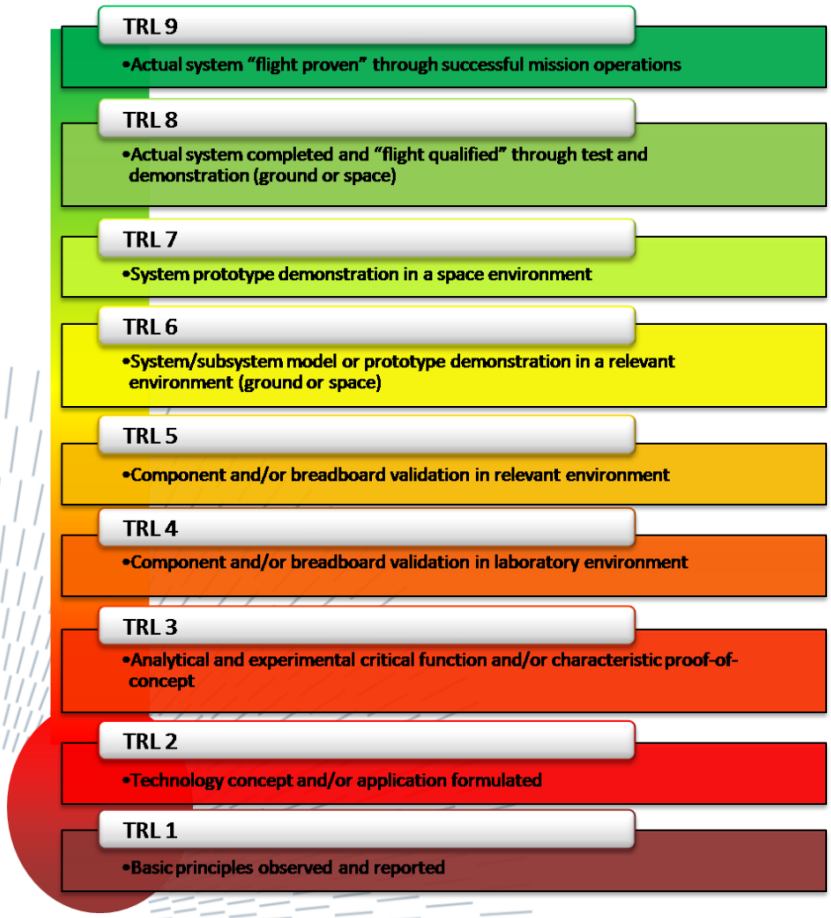

Figure 2: NASA's Technology Readiness Levels [4]

The present master thesis work describes the process of mechanical design and analysis of the prototype RF communications puck to be deployed and tested through ice in an analog Earth environment.

An ideal through-ice testing scenario in an analog Earth environment would be costly to implement. One approach would be to place one puck in a deep (>1000 m) ice borehole, place a second puck at the same depth in a parallel borehole several kilometers away, allow them to freeze in place, and then conduct transmission tests. The creation of deep ice boreholes that could accommodate the diameter of the PARTI prototypes is possible, but currently lies within the realm of large-scale Antarctic research projects. Common and naturally occurring features called moulins offer an alternative. Moulins are vertical, well-like shafts within glacier ice that form when summer meltwater streams on a glacier surface encounter a weak spot in the ice and begin to incise down to the glacier bed. In the autumn the streams cease to flow and the empty shaft of the moulin remains.

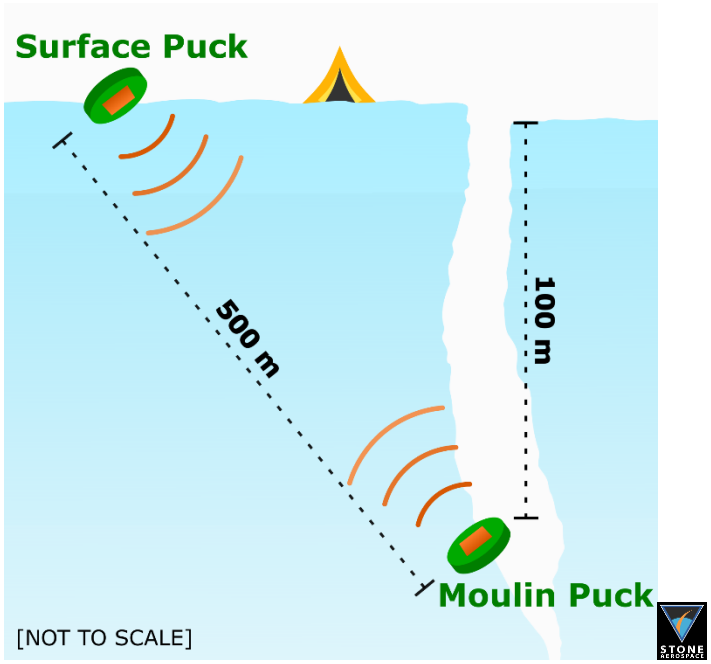

Figure 3: In-ice testing of the UHF and HF antenna puck designs can be accomplished by using a moulin as a natural ice well

Utilizing a dry moulin the Stone Aerospace field team will place a single puck against a moulin wall at a depth of ~100 m from the ice surface, and then embed a second puck at some distance from the moulin entrance on the surface, as shown in Figure 3. The surface puck will be successively embedded at several locations with differing path distances and elevation angles.

1.2 Aim and Scope of the Project

The present master thesis work describes the process of design and analysis of a prototype puck to be deployed in a moulin, to advance radio transceiver technology designed for cryobot missions.

For this development, both the patch antenna and the crossed-loop antenna were built with a size and weight that could be used in a flight puck. The puck hardware design adheres to realistic diameter for a landed mission to Europa, which is based on the cryobot available internal space of 30 cm. The height of the puck is freely adjusted to accommodate the commercial-off-the-shelf (COTS) electronics that drive the antennas.

The prototype puck must protect the electronics inside from the cold and wet environment and must ensure the electronics operational temperature range. The materials of the enclosure must be carefully selected not to interfere with the RF signals, and the enclosure must facilitate handling and operation in a harsh environment.

1.3 Prior Art

To date, only theoretical investigations of puck radio transceivers specifically designed for a cryobot mission have been conducted [5,6,7]. Nonetheless, there have been several notable projects that have addressed elements of wireless through-ice communications for tracking and data transfer. One such project is the Stone Aerospace VALKYRIE project, a cylindrical cryobot equipped with an ice-penetrating synthetic aperture radar, or IceSAR [8]. This look-ahead antenna was capable of detecting objects up to 125 m distance through the ice, operating at 0.75 GHz to 1 GHz. The backend hardware utilized COTS components that allowed for a range of up to 1 km, although the range achieved during the Matanuska Glacier campaign was limited by loss (S11) of 8 to 10 dB at the antenna feed terminals. Signal averaging and fast switching isolation switches could improve the range to 2 km for the same endurance.

Other notable advancements, the Stone Aerospace ENDURANCE and ARTEMIS Autonomous Underwater Vehicles (AUVs) [9,10], operated under ice and carried custom-built tracking beacons that created a 3500 Hz vertical magnetic field directly over the vehicle. The ENDURANCE beacon had a transmit power of 1 W, allowing for tracking in real-time in Lake Bonney, an Antarctic freshwater lake perennially

covered with a 5 m thick ice cap. The location of the AUV was accurate to within centimeters and could have been tracked through much thicker ice. For tracking under the Ross Ice Shelf (RIS), the ARTEMIS AUV was equipped with a more powerful transmitter, to overcome anticipated challenges such as brine layers above and saltwater below the vehicle. Despite obstacles like saltwater intrusions and a 6-meter-thick layer of accumulated platelet ice, the vehicle's location could be pinpointed to within a 1-meter circular error probable through as much as 14 meters of sea ice.

Moreover, during the ARTEMIS deployment, an experimental RF through-ice data telemetry test took place using a 10-meter-long insulated antenna, which communicated with a surface base station by transmitting 10 W at 2 MHz. Though this trial did not succeed due to a 10-meter-thick platelet ice layer, it remains a potential method in regions without platelet ice. In another test, a signal was detected nearly 1 kilometer away through platelet ice.

Also noteworthy are efforts such as the WiSe project [11], the Glacsweb program [12], and the Cryoegg project [13], which focused on deploying wireless sensor platforms for subglacial telemetry. These projects involved small probes, with the WiSe measuring 50 mm in diameter and 300 mm in length, the Glacsweb slightly larger at 68 mm, and the Cryoegg at 120 mm. The design of these prototype housings was mainly influenced by pressure conditions in the ice boreholes, making them distinct from the current thesis. These probes were designed for passive deployment, without the necessity for interaction or user interfaces.

Figure 4: Glacsweb probe, with electronics and sensors housed in a 68 mm diameter plastic egg-shape capsule made of two halves permanently bonded [12]

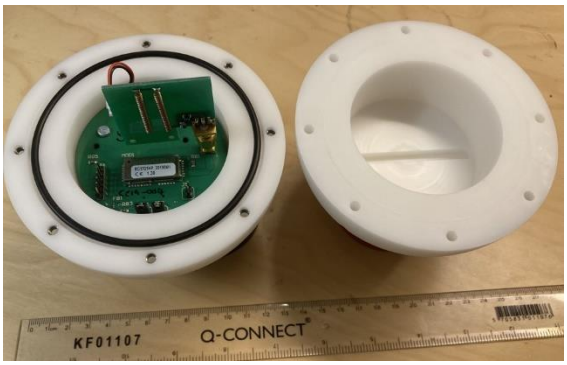

Figure 5: Cryoegg probe, made of two halves of machined acetal copolymer sealed with an O-ring and eight machined screws [13]

Among these, the Cryoegg probe bears the most resemblance to the subject of the present thesis. Cryoegg employs a low-frequency radio communication system at

30.3 MHz with On-Off Keying modulation, capable of transmitting data from subglacial environments to the surface at a rate of 10 bits per second. This enables real-time monitoring of parameters like pressure, temperature, and electrical conductivity. Cryoegg features a spherical enclosure made of acetal copolymer, split into two halves, and sealed with a rubber O-ring fastened by eight screws.

The aforementioned projects present notable advancement in subglacial research technology, particularly in communication systems. Their contributions serve as valuable reference points for the future advancement of subglacial exploration. The present thesis strides to contribute to the advancement of RF communication technology development, specifically tailored for cryobot missions, by employing advanced mechanical design methods and analysis to engineer a prototype puck suitable for testing in an analog environment.

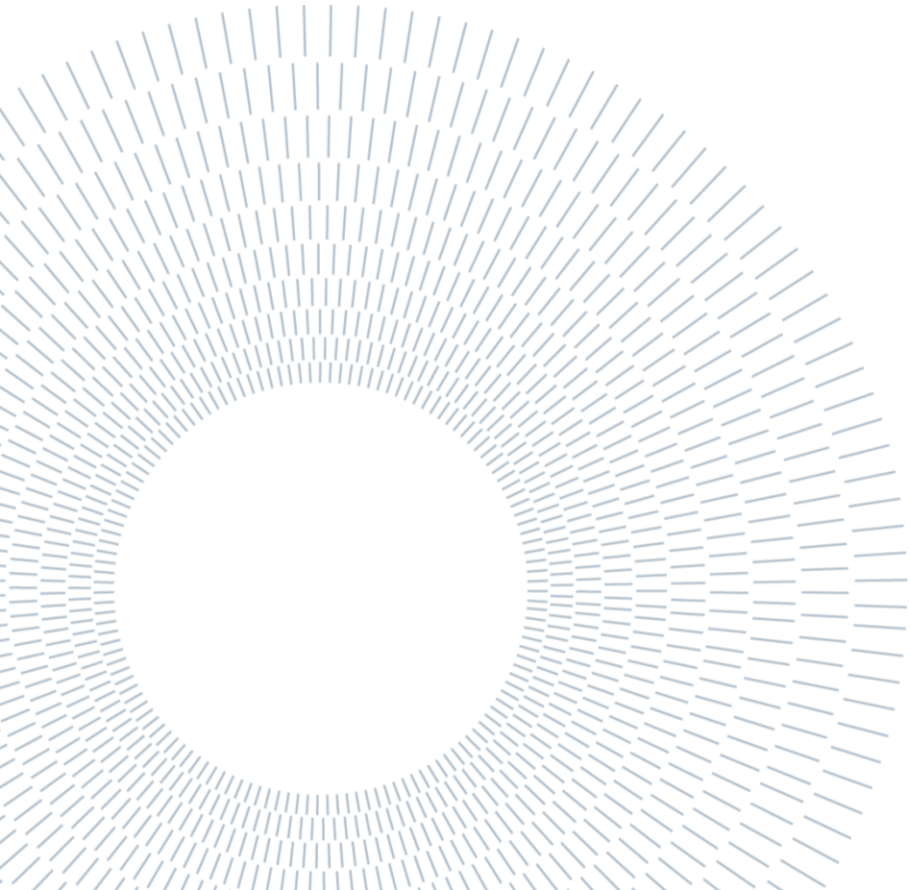

2 Requirements and Considerations

Prior to starting any design work, it is crucial to have well-defined requirements, as they serve as the targets for the final product. Additionally, a comprehensive understanding of the project considerations that could influence the design process is indispensable, including design priorities and final field-testing procedures. This section forms the foundation for the design process.

2.1 Mission and Prototype Requirements

The PARTI-Pucks prototype stage proposed by Stone Aerospace focuses on technology advancement by testing in relevant environment, not yet delving into the challenges of a space environment or "flight-qualified" hardware. However, one must keep in mind the mission requirements for a future Europa lander mission even when only designing for Earth analog environments.

The PARTI-Puck prototype requirements are derived from the Europa mission requirements referring to operational and environmental conditions expected on a Europa mission. Instead, prototype requirements focus on in-ice field test conditions expected in the analog Earth environment. Therefore, the prototype requirements drive the technical details of the prototype designs.

Table 1: Mission and Prototype Requirements

Cat.	Requirement	Mission Puck: Europa	Justification	PARTI-Puck: Moulin	Justification
System	Size, Diameter	**30 cm**	Cryobot internal usable diameter	**30 cm**	Based on mission-ready puck-sized antennas
	Size, Length	**55 cm total**	Length estimate of stack of pucks from previous cryobot system studies	**None**	Freely adjusted based on internal components

	Life Duration	**10 years+**	3 years of ice penetration plus multiple years of ocean exploration	**3 weeks**	Deployment duration
Environment	Operating Temperature	**-180 to 0 C**	Estimated Europa temperatures from the surface to the ocean	**-20 C to 10 C**	Expected operating temperature in Moulin
	Operating Pressure	**10^{-12} to 280 bar**	Vacuum during space travel and high pressures once embedded in Europa's ice shell	**1 bar**	Atmospheric pressure, no complete ice embedment
	Ingress Protection	**IP68**	Dust tight, water immersion beyond 1m	**IP64**	Dust tight, splashing water. No immersion in water or ice
	Radiation Protection	**Low**	Minimum Europe puck embedment is 1 meter under ice, where radiation is attenuated	**None**	No radiation concerns in Moulin field testing
	Planetary Protection	**10^{-4}**	Maximum probability of contamination	**None**	No life detection systems deployed
Power	Power Source	**Miniature RPS**	Integrated miniature radioisotope power system	**Battery surrogate**	Internal or external battery designed to match characteristics of the RPS
	Power Consumption	**1-3 Watts**	Low power	**1-3 Watts**	For running antennas.
Communications	Data Transmission Rate	**5 MB/day**	Target transmission rate for a mission	**0.5-5 kbps**	Target transmission rate for testing
	Bit Error Rate Maximum	**1.00^{-5}**	Over the ambient temperature range anticipated in Europan ice.	**1.00^{-5}**	Over the ambient temperature range anticipated during testing

2.2 Design Considerations

Given that the primary goal of the PARTI-Pucks project is technology advancement, the project's final goal is the demonstration of radio frequency communication through ice. The design considerations for the mechanical design of the pucks differ from those of a flight-ready device or mass-produced items due to the specific nature and low production quantities of the pucks. In total, four pucks were produced, with a life duration corresponding to the three-week field deployment for ice testing. The testing involves rappelling into an inactive moulin and attaching the puck to the ice in a cold, wet, and low-light environment.

The following are the design considerations defined along with Stone Aerospace and categorized into three groups according to their priority for the design and building process.

2.2.1 High-Priority Design Considerations:

- Function: The main objective of the mechanical development of the prototype puck is to safely house the antennas and associated electronics, protecting them from environmental factors and fulfilling the requirements stated in the previous section.
- Safety: The mechanical design must facilitate the transportation, installation, and operation of the puck in the field deployment. Additionally, it must protect the operator from electrical and thermal risks associated with the device.
- Manufacturability: To manage costs, all parts should be made from commercially available and easily accessible materials.
- Easy to Disassemble for Service: In case the puck does not perform as expected during tests, the electrical systems and antennas may need to be checked. Therefore, the puck must be designed for easy opening and servicing in a tent on a glacier. The internals should be arranged in a way that allows for effortless servicing. Conversely, assembly and disassembly for end-of-life are not top priorities, as these operations will be conducted in a lab with a wider range of tools and time available.
- Field Non-Contamination: All components must be removable, leaving no permanent trace in the glacier. In a real flight mission, cryobot systems must adhere to planetary protection measures.

2.2.2 Medium-Priority Design Considerations:

- Size: The outer diameter of the puck is constrained by the cryobot's internal usable diameter, at 30 centimeters (approximately 11.81 inches). The height, however, is a more flexible design variable. Nevertheless, it should be kept as small as possible to facilitate transportation to Greenland and down the moulin.
- Weight: Similar to size considerations, the weight of the puck should be minimized to ease transportation by a courier on rappel, as one puck will be hand-carried down the moulin.

2.2.3 Low-Priority Design Consideration:

- Sustainability: Although sustainability is a low priority for this project due to the minimal production quantities, it should be considered primarily through the choice of materials, manufacturing processes, and design for end-of-life. With only four pucks being produced, the impact on sustainability is minimal but should still be acknowledged in the design process.

In summary, the mechanical design of the radio frequency communication pucks for ice environments should prioritize function, safety, manufacturability, ease of disassembly for service, and field non-contamination. Medium priority should be given to size and weight considerations, while sustainability, although a low priority, should still be acknowledged through material selection, manufacturing processes, and end-of-life design. By adhering to these design considerations, the project can successfully develop a technology that is both advanced and suited to its intended environment.

2.2.4 Field Testing

The mechanical design of radio frequency communication pucks must consider the harsh conditions encountered during field testing. These conditions include extreme cold, handling with gloves, potential hanging from ropes, and the absence of a stable floor. The design of the pucks should account for these challenges, ensuring that all switches and indicator lights are intuitive and easy to reach, and that the prototype has rigging points and surfaces to attach to the ice and stay in place during communication testing.

To advance the radio frequency communication puck designs to Technology Readiness Level (TRL) 5 and address elements of TRL 6 qualification, a link test measuring data rate and signal strength through 500 meters or more of ice with the pucks in contact with the ice is required. However, an ideal through-ice testing

scenario in an analog Earth environment would be costly and challenging to implement.

A more feasible approach involves the use of moulins, which are vertical, well-like shafts within glacier ice that form when summer meltwater streams on a glacier surface encounter a weak spot in the ice and begin to incise down to the glacier bed. In the autumn, the streams cease to flow, and the empty shaft of the moulin remains. Utilizing a dry moulin, a single puck can be placed against a moulin wall at a depth of approximately 100 meters from the ice surface. A second puck is then embedded at some distance from the moulin entrance on the surface. The surface puck is successively embedded at several locations with differing path distances and elevation angles. This allows for the evaluation of antenna coupling for various surface grazing angles and propagation path inhomogeneities. Such tests provide the most complete and relevant means of assessing the mechanical design of the pucks within ice.

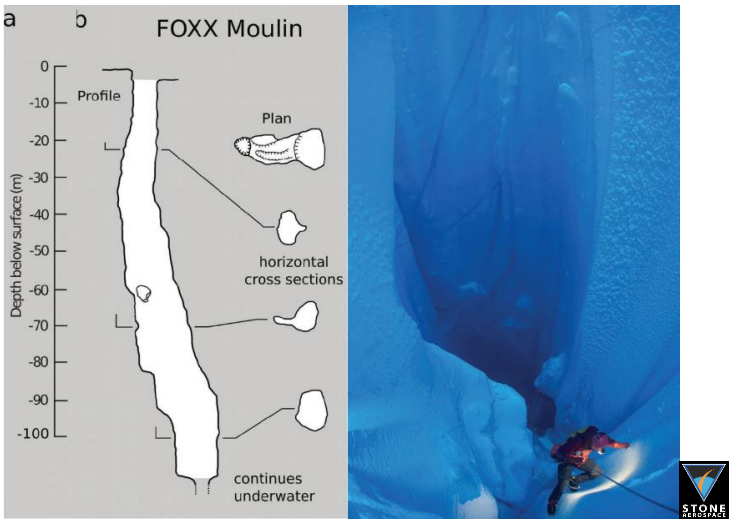

Figure 6: FOXX Moulin profile map shows the feature has been mapped to over 100 m depth (left). A researcher investigates FOXX Moulin in 2019 (right, photo credit J. Gulley)

Clean, debris-free ice and a deep moulin within thick ice (far removed from the glacier bed) are preferable for field testing. These conditions are uniquely met on the Greenland Ice Sheet. FOXX Moulin, a persistent feature located on the western margin of the ice sheet, can be reached by a 30-minute Air Greenland helicopter flight from the international airport in Ilulissat. Since 2012, FOXX Moulin has been the subject of a series of NSF-funded investigations performed by glaciologist Dr. Jason Gulley and others, making it a suitable site for testing the performance of radio frequency communication pucks.

In conclusion, the mechanical design of radio frequency communication pucks must consider the extreme conditions encountered during field testing. The design should prioritize ease of use, accessibility of components, and secure attachment to the ice. By utilizing natural features like moulins, the field testing can provide valuable insights into the performance and adaptability of the pucks under harsh environmental conditions, informing further design iterations and improvements.

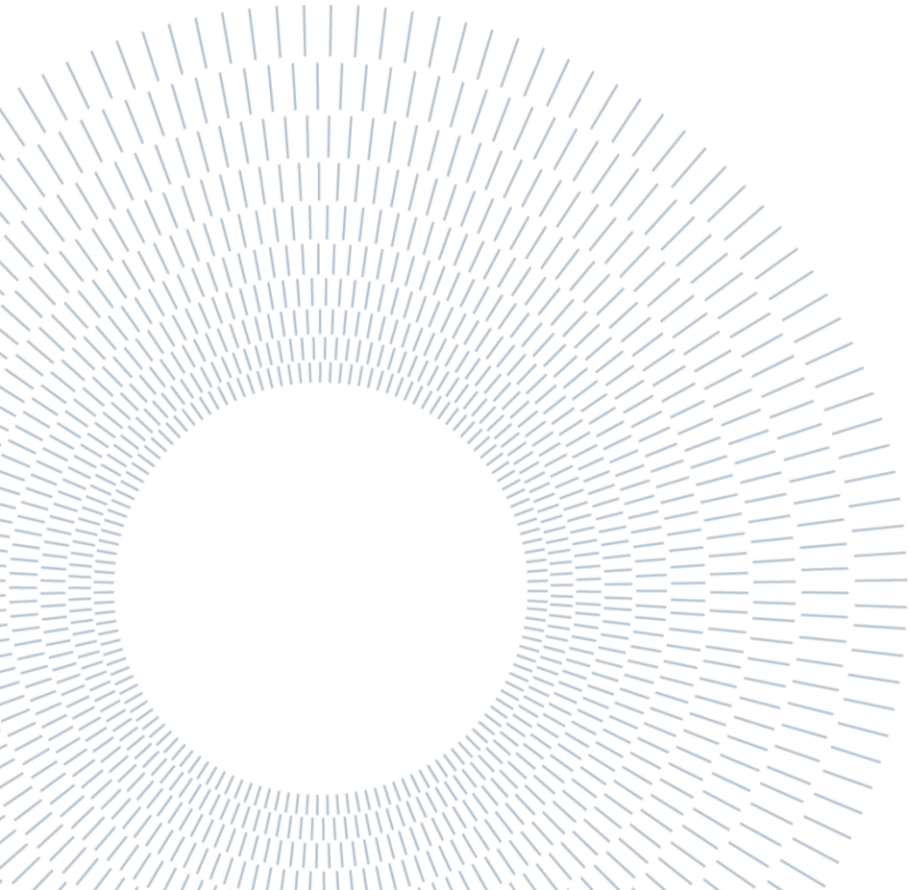

3 Preliminary Design

In the preliminary design phase of the radio frequency communication pucks, initial plans involved creating two separate puck designs: one for the patch and antenna, and another for the crossed-loop antenna. Despite sharing the same electronics and housing requirements, these designs were originally conceived as distinct entities. However, it was soon determined that combining both antennas into a single unified puck design would be advantageous, as this would not only eliminate hardware redundancy but also simplify field operations.

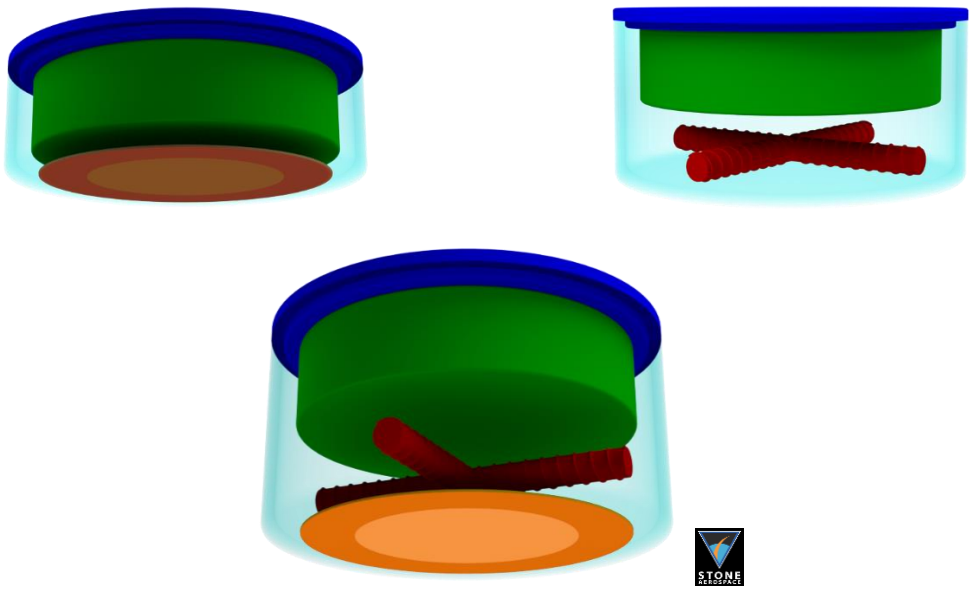

Figure 7: Preliminary design of the prototype pucks. Initially involving two separate puck designs: one for the patch antenna (top left) and another for the crossed-loop antenna (top right), and later on transitioning to a unified prototype puck (bottom)

Components: housing in light blue, lid in dark blue, electronics in green, patch antenna in orange, and crossed-loop antenna in red.

Another critical decision made during the early stages of the design process was to maintain the battery as a separate component from the puck. This decision was based on two primary factors. First, the battery underwent its own design phase, which

involved selecting the appropriate chemistry, configuration, and size. Decoupling the battery design from the puck allowed for greater flexibility in addressing these individual design considerations. Second, by keeping the battery separate, the overall size and weight of the pucks could be reduced, contributing to easier transportation and handling during field testing.

3.1 Patch Antenna

The patch antenna, developed by the PARTI-Pucks team at University of Colorado, serves as the primary communication component for the VHF/UHF range in the radio frequency communication puck. This circular antenna features circular polarization, a frequency of 413 MHz, and a radiation efficiency of 70-80%. Its design is straightforward, consisting of a microstrip patch antenna on a ground plane separated by a dielectric. A software-defined radio (SDR) is employed to manage the frequency of the transmitters and receivers.

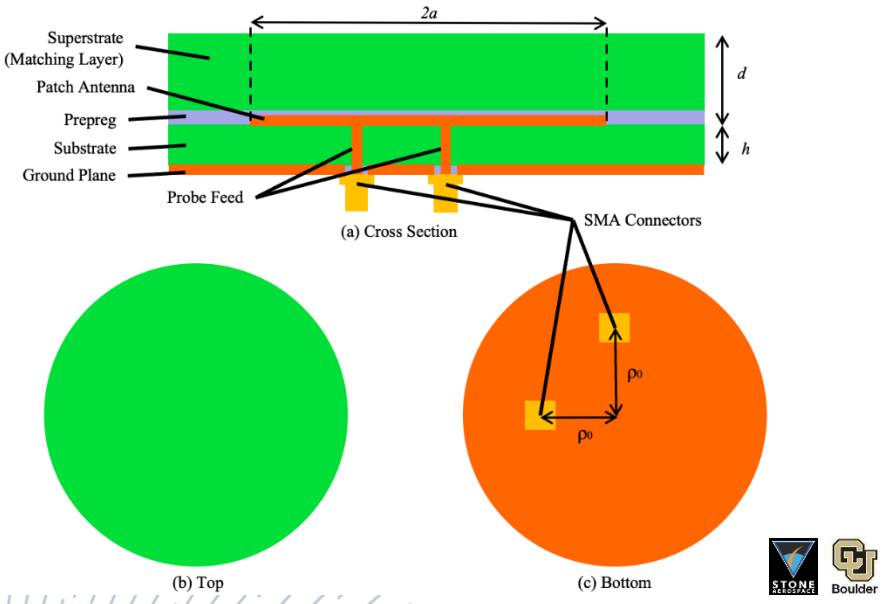

Figure 8: UHF Patch Antenna Design

To ensure optimal communication, the patch antenna must be in direct contact with the ice, minimizing the air gap between the antenna and the ice as much as possible. It is crucial to prevent any water layer from forming in front of the antenna, as this would significantly impact the radiated signal.

Figure 9: UHF Patch Antenna assembled on the bottom side of the puck housing

From a mechanical standpoint, the patch antenna is situated on the ice-facing side of the puck housing, or the bottom side of the prototype to maintain close contact with the ice. It is securely attached using #10 flat head screws and an appropriate adhesive compound for water sealing. Two SMA cables connect to the back of the patch antenna PCB, providing service loops for easy internal connection and access. The patch antenna is designed to protrude slightly, approximately 1 mm above the surrounding surface, ensuring direct contact with the ice during operation.

3.2 Crossed-Loop Antenna

The crossed-loop antenna serves as the primary communication component for the HF range in the radio frequency communication puck. Constructed from 7/8" diameter ferrite rods, the crossed-loop antenna features one solid rod and another split with saddle joints in the middle, forming a 10" by 10" cross. A 90-degree phase shift network between the loops generates up/down circular polarization. Each rod is wrapped with #16 AWG enameled magnet wire and comprises two 7-turn counter-wound windings in parallel, designed for a 5MHz RF signal. The low number of turns maintains low impedance and transmit voltage, while the counter-wound windings in parallel effectively cancel most of the electric field, optimizing the antenna pattern.

To prevent interference, the crossed-loop antenna must be situated at least 1" away from the patch antenna and large electronics. This distance was determined through

impedance testing to ensure optimal performance without compromising the functionality of other components within the radio frequency communication puck.

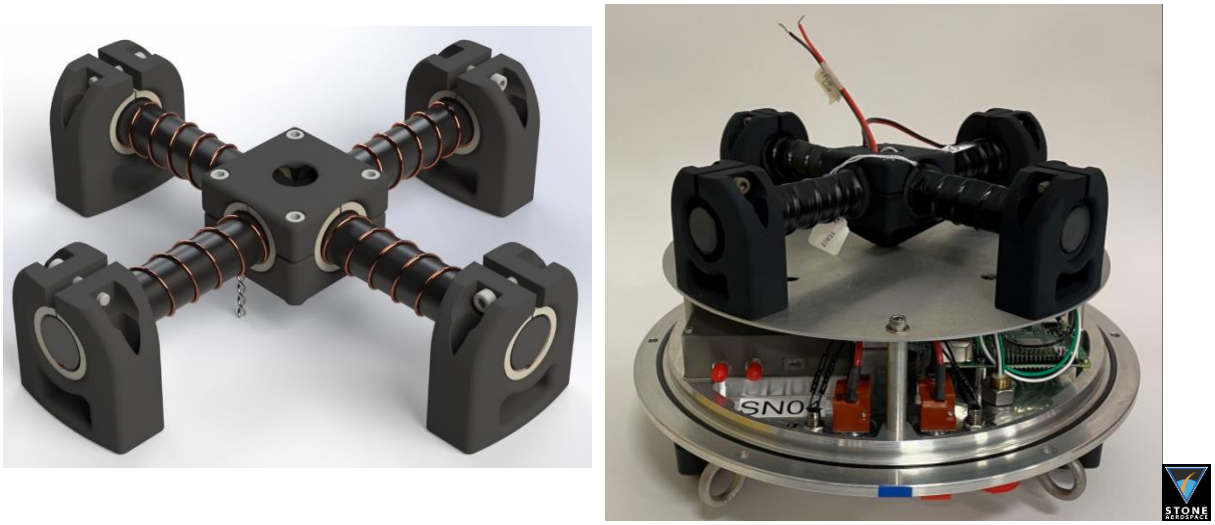

Figure 10: Rendering of the HF Crossed-Loop Antenna subassembly on the left, and picture of the subassembly attached to the puck lid through the five supporting standoff clamps, maintaining a one-inch distance from all other components

3.3 Electronics

A significant portion of the internal space within the radio frequency communication puck is occupied by various electronic components. These include a microcontroller unit (MCU, a Raspberry Pi), a software-defined radio (SDR, a HackRF One), a custom RF Feed, Amplification and Matching Network (FAM) PCB, and a custom power conversion board. Furthermore, it is essential to enclose the SDR and the circuits on the FAM board in Faraday shields to ensure proper RF isolation and prevent interference with other components in the system.

3.4 User Interface

The User Interface is situated on the side opposite the patch antenna, specifically on the exterior lid surface at the top of the prototype puck. This area houses switches, cables, LED indicators, and hardware mounting points for easy accessibility. It is important to note that in a mission-ready puck system, these components would not be present, as the cryobot would be deployed without any need for user interaction with the pucks. Consequently, the space occupied by the User Interface in the prototype puck would be eliminated.

Figure 11: View from the top of the puck, looking at the User Interface on the lid

3.5 Preliminary Design

The initial design presented at the project's preliminary design review meets all the requirements mentioned in Section 2.1 and serves as a starting point for the design work and analyses presented in the following sections. This initial design showcases a lid and a housing made from plastic for RF transparency and sealed with an O-ring radial seal on the lid.

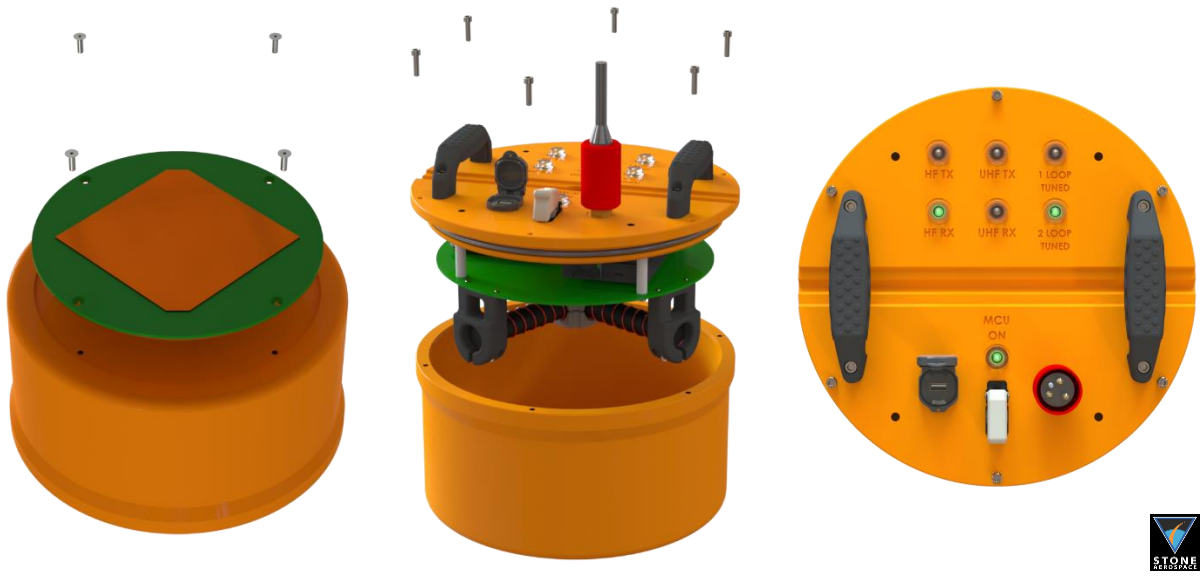

Figure 12: Multiple views of the preliminary design of the prototype puck

The patch antenna sits on a recess at the bottom of the housing, and it is attached by four flat head screws.

Looking at the puck internals, the crossed-loop antenna is attached from five supporting points to the FAM board, the green circular board. The standoffs on the edges of the crossed-loop are clocked close to the white standoffs that connect the FAM board to the lid. The rest of the electronics sit between the FAM board and the lid, using both mounting surfaces.

The outside lid surface has an LED display zone at the top, with the indicator lights spread out around the surface, a bottom zone with connectors and switches, COTS handles on the sides and a strap groove running horizontally below the handles.

4 Detailed Design

In the detailed design section, we present an in-depth examination of the mechanical design aspects of the radio frequency communication puck, also known as the PARTI-Puck. This prototype features a modular design, 30 cm in diameter by 22 cm in height, consisting of four main sections, listed from top to bottom, that slightly differ from the conceptual design:

a) Lid and Electronics assembly, shown in blue in Figure 13. This subassembly also includes the user interface on the lid outside. The electronic boards are located on the lid inside.
b) FAM Board assembly, shown in green. Formed by the RF Feed, Amplification and Matching Network and its EMI shielding.
c) Crossed-Loop Antenna assembly, shown in red. Includes the antenna and fixturing components.
d) Housing and Patch Antenna assembly, shown in orange. The antenna sits on the bottom side of the housing for direct contact with the ice.

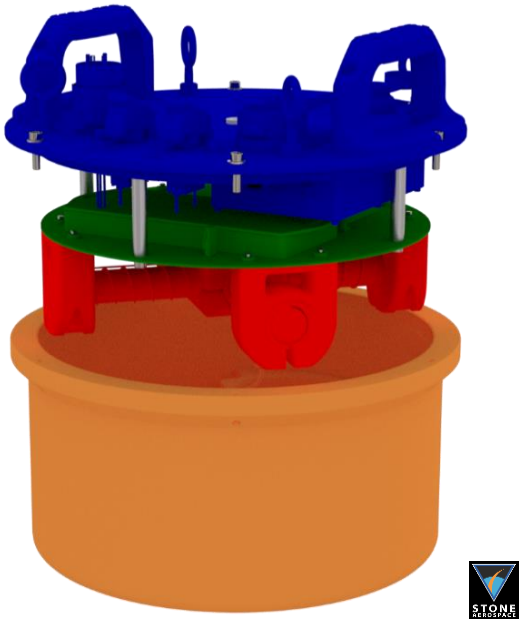

Figure 13: Diagram of the prototype puck showing the four main sections of the design in different colors

The mechanical design has been tailored to address the unique challenges posed by the harsh testing conditions, such as low temperatures, glove handling, and the necessity of secure attachment to the ice. This section explores the design decisions and component arrangements that ensure efficient performance, safety, manufacturability, and ease of maintenance, all while adhering to the size, weight, and sustainability considerations outlined in the design priorities.

4.1 Design for Manufacturing

Each final prototype puck is made from 116 unique parts, and a total of 230 total part count. From the total part count, they can be divided into three main categories: antenna-related components, electronics and mechanical components, where the mechanical components represent 69% of the total part count.

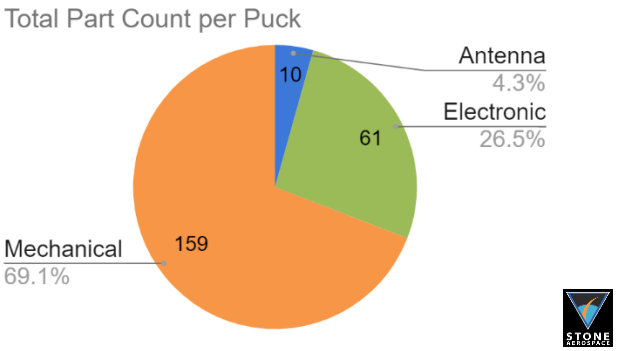

Figure 14: Pie chart of the total part count in a puck per component category

From the mechanical components, over 80% of them are fasteners, while 11% are custom parts, and the remaining components are Commercial Off-The-Shelf (COTS) parts excluding fasteners.

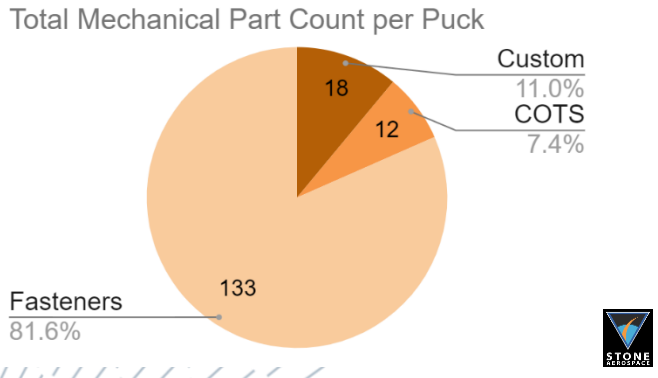

Figure 15: Pie chart of the part count of mechanical components in a puck per category

4.1.1 Bill of Materials

In this subsection of the present thesis, we will delve into the composition of the four primary subassemblies and the components constituting each. Serving as a foundation, this exploration will serve as a baseline to further discuss the selection of manufacturing processes and materials, the incorporation of design features,

considerations for ease of assembly, and the execution of structural and thermal analyses. Through this systematic approach, we will achieve a comprehensive understanding of the various elements and the intricacies of their integration within the puck assembly, setting the stage for more in-depth analyses in the following sections.

The Lid and Electronics assembly is composed of a machined aluminum lid which features field components on the top surface and electronic boards on the bottom surface. The electronics are strategically mounted directly onto the lid to promote efficient heat dissipation from the interior of the puck. The electronic components integrated into this assembly include the Interface Board, the Raspberry Pi, and the HackRF One, which is securely housed within a conductive EMI enclosure.

Furthermore, on the top surface, the LEDs provide critical information regarding the status of the puck. Two switches control the main computer and power, complemented by a power connector and a data connector. For handling and secure attachment, four eyebolts are included, as well as a Disto-X adapter, which is instrumental in verifying the correct orientation of the puck. Further details regarding the top surface components can be explored in the User Interface section.

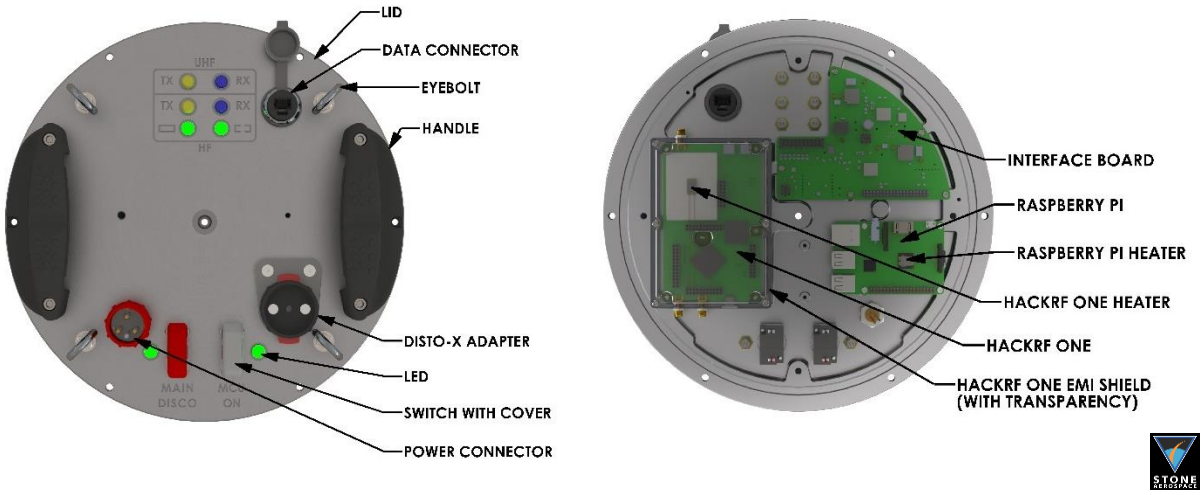

Figure 16: View of the top and bottom surfaces of the Lid and Electronics Assembly with component labels

The FAM Board assembly is composed of a circular FAM board, which incorporates both HF and UHF circuits. These circuits are shielded with EMI barriers to prevent electromagnetic interference. The EMI shields comprise a brass base that is soldered firmly to the board, coupled with a 3D-printed lid. The lid is treated with a nickel coating and features a carefully designed snap-fit mechanism that securely attaches it

to the brass box and ensures contact every centimeter apart. Additionally, conductive EMI foam gasketing is strategically placed between the box and the lid to ensure optimal shielding.

The assembly features a heater, which maintains the desired temperature levels and ensures the operation of the FAM board in various environmental conditions. Moreover, the assembly incorporates PEM® inserts for circuit boards to securely attach the crossed-loop assembly.

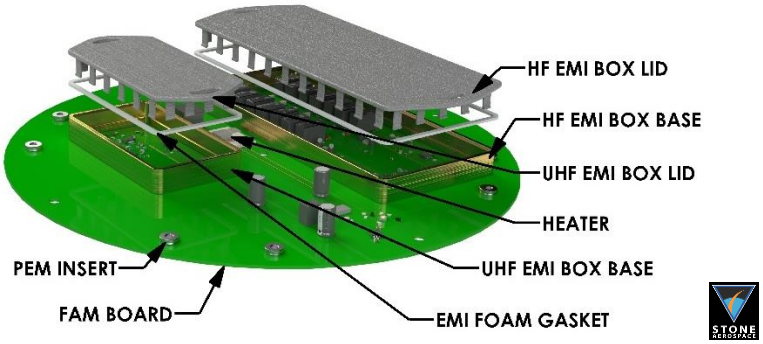

Figure 17: Exploded view of the FAM Board assembly with component labels

The Crossed-Loop Antenna assembly consists of the crossed-loop that is securely attached at five distinct points, ensuring structural integrity during potential impacts or drops. Since the crossed-loops are handcrafted, and the ferrite material is brittle, the standoffs are engineered with flexibility to accommodate the dimensional tolerances and protect the antenna. Shock-absorbing foam is strategically placed between the antenna and the oversized standoff holes. It is important to highlight that the fasteners used in this assembly PEEK screws. This choice is critical, as their proximity to the antenna requires a material that does not interfere with the antenna's functionality.

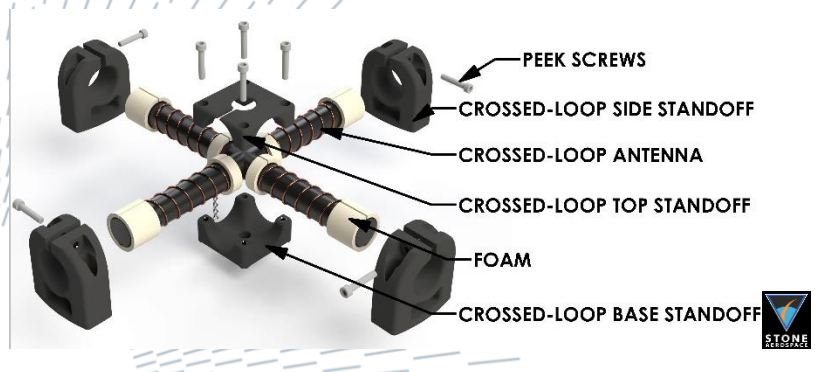

Figure 18: Exploded view of the Crossed-Loop Antenna assembly with component labels

The Housing and Patch Antenna assembly, as the name indicates, is primarily formed by the housing and the patch antenna, along with the antenna face insulation foam, the SMA cables and eight flat head Nylon screws that mechanically secure the patch antenna to the housing.

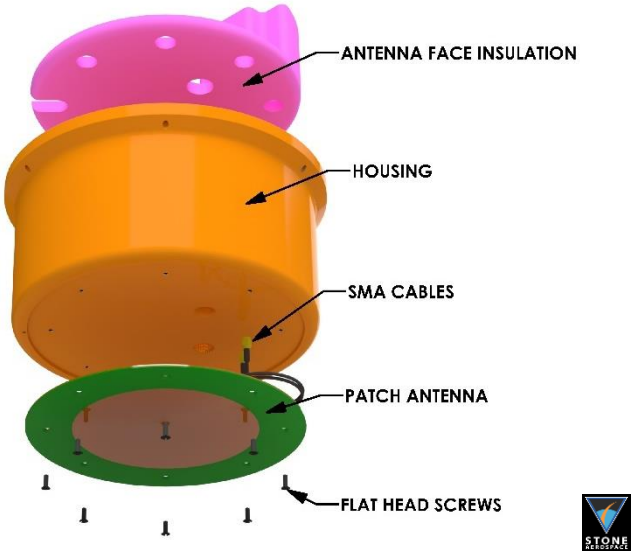

Figure 19: Exploded view of the Housing and Patch Antenna subassembly with component labels

The housing is made from 3D printed ULTEM, with helicoils installed for the fasteners from the antenna and from the lid assembly. Other notable features of the housing are the patch recess at the bottom for a flat profile, and the two openings at the bottom for the SMA cables to pass through before getting sealed with epoxy for waterproofing.

The patch antenna is secured in place with epoxy and eight plastic flat head screws to avoid possible warping. The antenna face insulation serves both as a thermal barrier from the heat emitted by the electronics and for cable management. The tall feature shown in Figure 20 guides the SMA cables to neatly coil while lowering the rest of the puck assembly.

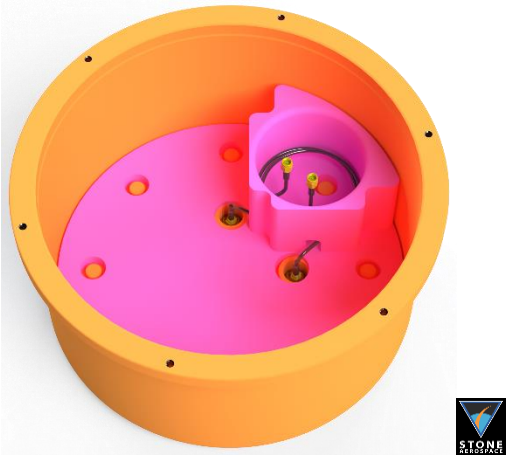

Figure 20: Top view of the Housing and Patch Antenna assembly, showcasing the SMA cables neatly coiled inside the insulation foam

4.1.2 Custom Components: Design and Material Selection

Within the puck assembly, custom components, although constituting a minor fraction in terms of the total number of parts, account for more than half of the total hardware cost. An iterative design process was employed in the design phase to select the most appropriate manufacturing process and material. Additionally, it involved designing features that not only fulfill the desired functionalities but also align with the project's objectives, all the while ensuring cost efficiency.

Figure 21 presents a detailed exploded view of the puck assembly, with an emphasis on the custom mechanical components. These components can be classified into four categories according to their specific roles:

- Base components: This category includes the lid and housing, which are essential elements in the construction of the puck. Their design is critical to the integrity and functionality of the assembly.
- EMI Mitigation components: These are designed as seamless shields made of conductive materials or coatings to effectively block electromagnetic fields, safeguarding the electronics within the assembly from electromagnetic interference.
- Structural Components: This category encompasses components such as the crossed-loop antenna standoffs and handle spacers. These play a crucial role in securing components in place and facilitate handling in field operations.
- Insulation: The insulation components are integral to thermal management, ensuring that the puck assembly maintains optimal temperatures, especially in extreme environments.

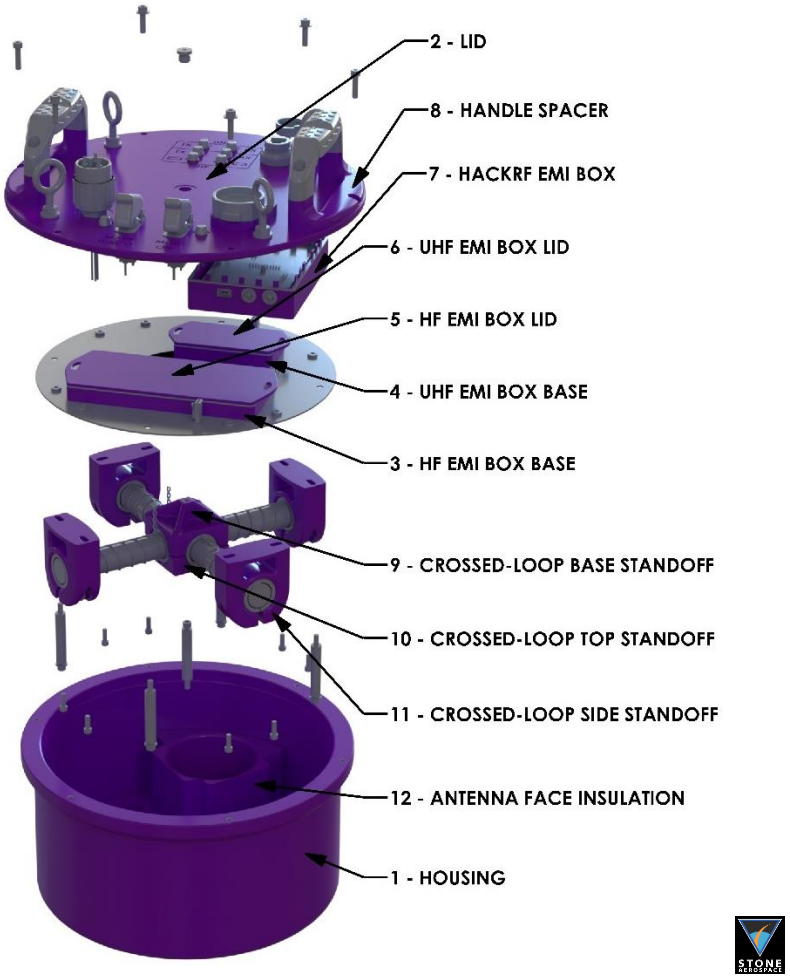

Figure 21: Exploded view of the puck assembly, showing the custom mechanical components in purple

The table presented below offers a detailed breakdown of the custom mechanical components, organized by category. For each component, the table specifies the manufacturing process employed, the material from which it is made, and the associated cost. This information is essential for understanding the rationale behind the choices made during the design phase and provides insights into the economic considerations involved in the creation of these components.

Table 2: Custom mechanical components by category, detailing manufacturing process, material and cost

Item	Part	Qty per puck	Category	Process	Material	Cost ($/part)	Total cost ($/puck)
1	Housing	1	Base	3D Print + epoxy seal	ULTEM	2,140	2,140
2	Lid	1	Base	Machined	Aluminum	1,200	1,200
3	HF EMI Box Base	1	EMI mitigation	Machined	Brass	144	144
4	UHF EMI Box Base	1	EMI mitigation	Machined	Brass	107	107
5	HF EMI Box Lid	1	EMI mitigation	3D Print + coating	Nylon PA12	16	16
6	UHF EMI Box Lid	1	EMI mitigation	3D Print + coating	Nylon PA12	6	6
7	HackRF EMI Box	1	EMI mitigation	3D Print + coating	Nylon PA12	28	28
8	Handle Spacer	2	Structural	3D Print	Nylon PA12	3	6
9	Crossed-Loop Base Standoff	1	Structural	3D Print	Nylon PA12	12	12
10	Crossed-Loop Top Standoff	1	Structural	3D Print	Nylon PA12	7	7
11	Crossed-Loop Side Standoff	4	Structural	3D Print	Nylon PA12	17	69
12	Antenna face insulation	1	Insulation	Machined	Foamular	39	39

The material selection of the custom mechanical components is critical as it directly impacts the performance, durability, and overall efficacy of the system. Materials need to withstand the environmental conditions they are subjected to and perform reliably under these circumstances. Moreover, it is essential to consider aspects like cost-effectiveness, availability, and compatibility with other components. In this

section, we will discuss the rationale behind the selection of each material, explore their properties and how they contribute to the overall functionality and objectives of each component.

Table 3: Color-coded exploded view of the puck highlighting different materials utilized

- Nylon PA12: is a strong thermoplastic for functional prototyping and final parts. It is a high-density material with watertight properties. This material is used for the crossed-loop clamps, the EMI boxes and handle spacers, due to the material's strength, low density and ability to achieve complex shapes. Additionally, for the EMI box components, the Nylon PA12 is painted over with liquid nickel coating for achieving a conductive surface.
- Aluminum 6061-T6: is a common aluminum alloy with good workability, machinability, and corrosion resistance properties. This aluminum grade has mechanical properties suitable for structural components, and it is a lightweight metal. This material grade is used for the puck lid for its ability to machine repeatable and reliable O-ring surfaces through CNC machining.
- FOAMULAR: is a high-performing insulation, used at the bottom of the puck housing on the antenna face insulation for two purposes. The first is to keep the heat dissipated by the crossed-loop antenna and electronics from flowing towards the patch antenna at the risk of forming a water layer between the antenna and altering the RF signal transmitted. The second purpose of the insulation piece is to provide a contained space for the SMA cables going from the patch antenna to the FAM board to neatly coil and keep a distance from the crossed-loop for signal coupling mitigation.
- Brass 360: is one of the copper alloys with the highest machinability, and it is a highly conductive material. This material grade is used for the FAM board EMI shields, providing a sturdy base that is soldered directly to the board, and then

forming a closed conductive cage once the EMI box lids are put in place.

- ULTEM 1010: is a high-performance thermoplastic that offers excellent strength and thermal stability. This material is used for the puck housing, through the process of FDM 3D printing due to the large size of the part. This material is non-conductive and allows the RF signals to pass through. Additionally, the housing is coated with resin epoxy to improve the waterproofing of the part.

4.1.3 Fasteners: Material Selection

The selection of fastener materials is critical in ensuring the optimal performance under environmental conditions, meeting the requisite strength and thermal requirements, and avoiding any interference with the RF communication technology. The following are the five different fastener materials employed within the puck assembly:

- Stainless Steel, 316 (displayed in red in Figure 22): As a go-to material at Stone Aerospace for generic hardware, this grade of stainless steel is utilized for bolts that don't necessitate special properties, in addition to all washers, nuts, and the eyebolt on the lid. Stainless steel 316 offers the standard corrosion resistance, strength, and easy maintenance for which stainless is known.
- Stainless Steel, 18-8 (displayed in yellow): chosen for all helicoils in the assembly due to availability. This grade is employed when high corrosion resistance levels are not essential, making it a cost-effective alternative to 316. The helicoils' small size and proximity to the antennas do not affect signal transmission.
- Aluminum 6061 (displayed in blue): employed for the spacers between the FAM board and the puck lid. This aluminum grade offers excellent corrosion resistance, high-to-moderate strength, and great machinability. It was chosen for the spacers particularly for electrical and thermal conduction between the FAM board and the lid. The exposed ground layer on the FAM board allow the spacers to act as conductors to the chassis ground.
- PEEK (displayed in pink): this thermoplastic polymer is used for the bolts that tighten the crossed-loop antenna standoffs. As these bolts are situated close to the antenna and bear loads, PEEK's excellent tensile strength and non-conductive nature make it a great choice. Though expensive, the use of PEEK is deemed justifiable.
- Nylon (displayed in green): another thermoplastic polymer, Nylon is employed for the flat head screws that fix the patch antenna to the housing. It is worth noting that the patch antenna is primarily secured with epoxy, and

these screws serve as a secondary securing mechanism, placed towards the edges to counteract any potential warping of the antenna. Nylon's non-conductive properties and affordability make it suitable for low-load bearing bolts.

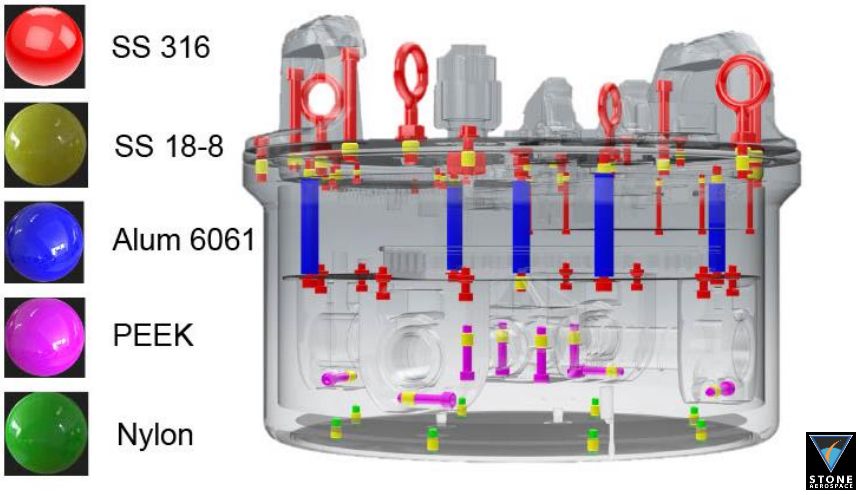

Figure 22: Color-coded transparent view of the puck highlighting different fastener materials utilized

4.2 Design for Assembly and Disassembly

In the Design for Assembly section, we will focus primarily on optimizing the disassembly process for serviceability, which is of paramount importance due to its repetitive nature throughout the product's life cycle. Additionally, it's vital to consider that this disassembly for serviceability will often be conducted in challenging environments such as glaciers, at remote field deployment sites where supplies are limited. Moreover, the field team, which might not have extensive knowledge of the mechanical design of the pucks, will perform these operations. From the early stages of design, careful consideration was given to streamline the assembly, but particular emphasis was placed on ensuring ease of disassembly for maintenance and repairs. In contrast to the initial assembly or the final disassembly at the end of the product's life, serviceability is a recurring need. Therefore, strategies to decrease disassembly time, reduce the number of tools and operations required, and simplify the overall process were integrated into the design. These tactics not only contribute to cost-efficiency but are also crucial in preserving the product's functionality and aesthetics, and ensuring practicality and adaptability under the harsh conditions faced in remote locations.

There are three main operations for disassembly for serviceability that may be required. Operation A involves opening the puck to separate the housing and lid assemblies, which is a prerequisite for any of the subsequent operations. Operation B entails detaching the FAM and crossed-loop assemblies from the lid assembly. Operation C involves separating the Crossed-loop antenna from the FAM board. It is worth noting that operations B and C can be executed independently. Meticulous planning ensured that each of these operations involves only two or three steps at most. To facilitate this process, an instruction manual has been developed to guide the field deployment team through the disassembly operations. The manual is designed to be user-friendly, allowing any member of the field deployment group to easily understand the instructions, identify the required tools, and execute the operations effectively.

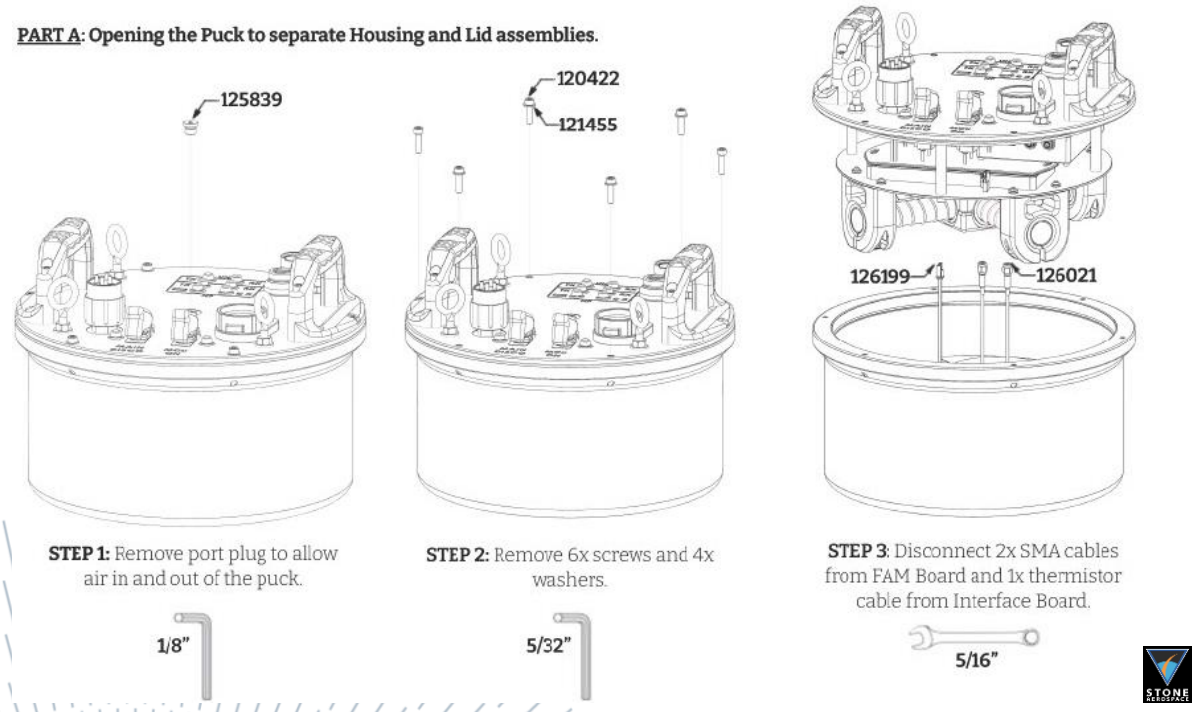

Figure 23: Disassembly for Serviceability instructions manual for Operation A, opening the puck to separate Housing and Lid assemblies

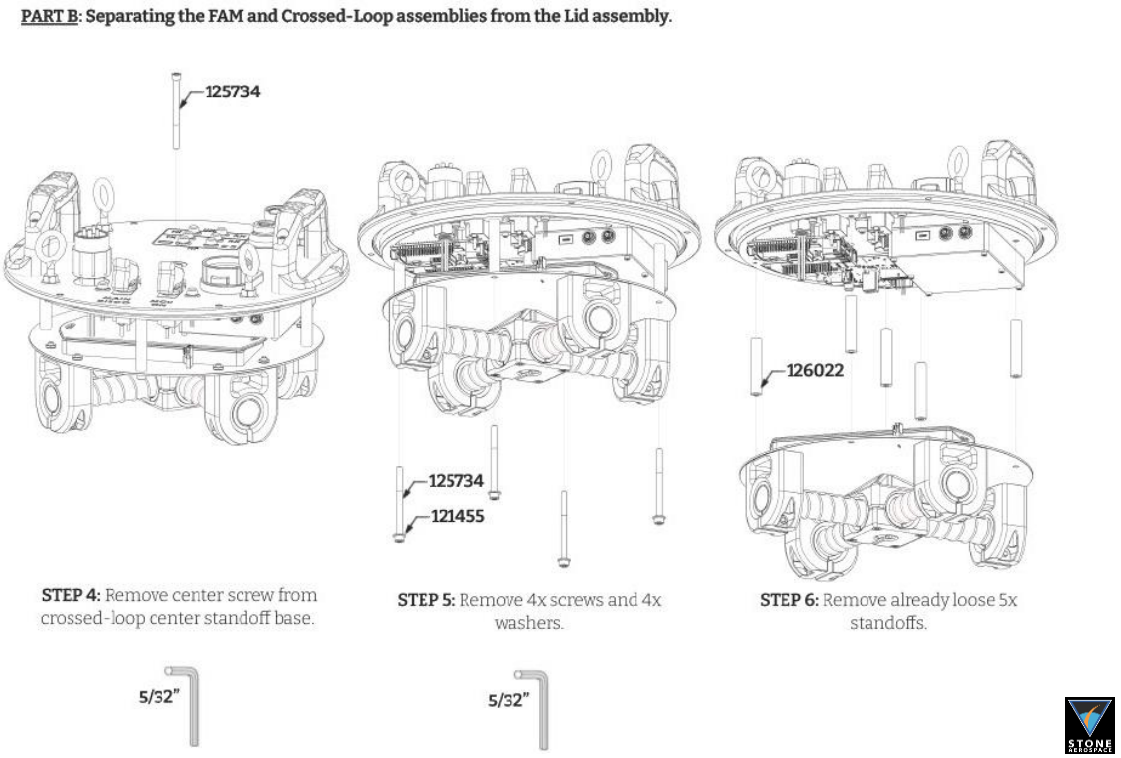

Figure 24: Disassembly for Serviceability instructions manual for Operation B, separating the FAM and Crossed-Loop assemblies from the Lid assembly

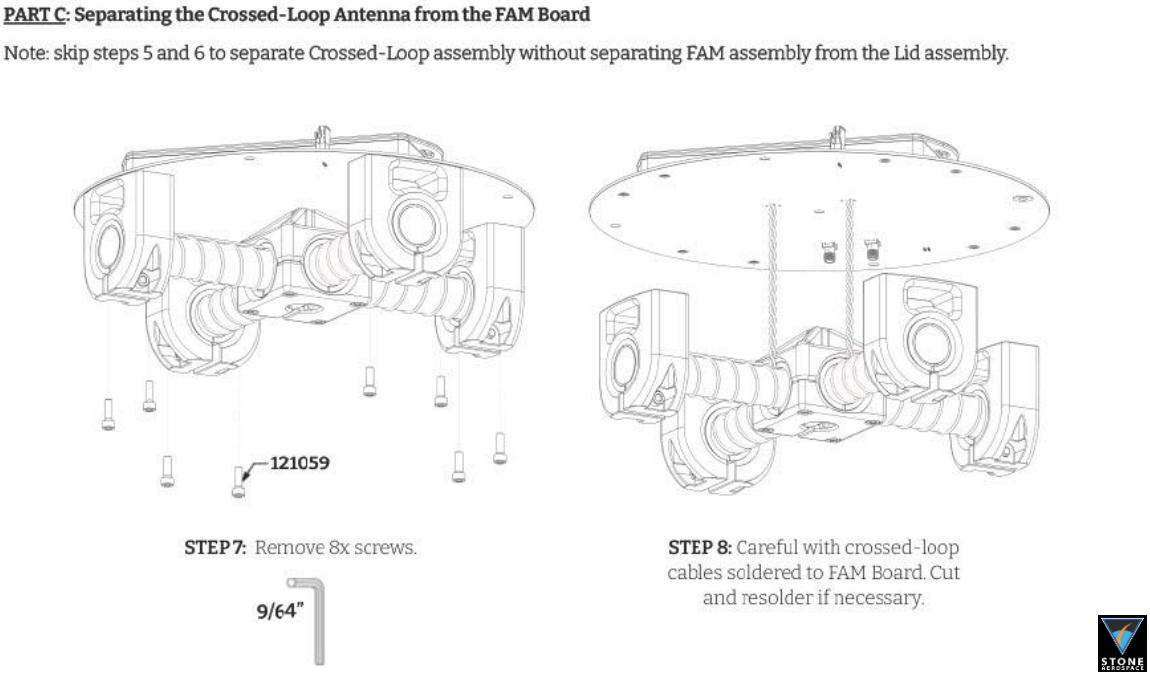

Figure 25: Disassembly for Serviceability instructions manual for Operation C, separating the Crossed-Loop Antenna from the FAM Board

For reassembly, the steps should be carried out in reverse order. The simplicity and efficiency of these operations were achieved through multiple iterations of the design, adhering to key design for assembly principles. These principles encompassed creating a modular design, reducing the number of parts, standardizing components, minimizing the need to reorient parts during assembly, and incorporating symmetrical designs for ease of insertion.

Moreover, a specialized Bench Jig assembly was devised to provide a stable and convenient platform for securing both the Lid and Housing assemblies. This jig is particularly useful during benchtop inspection or maintenance tasks. Figure 26 provides a visual representation of the Bench Jig in action, while Figure 27 illustrates the various orientations and applications that the assembly can facilitate. This arrangement not only enhances the ease of assembly and disassembly but also promotes precision and reliability during inspection or servicing processes.

Figure 26: Picture of the Bench Jig assembly in use

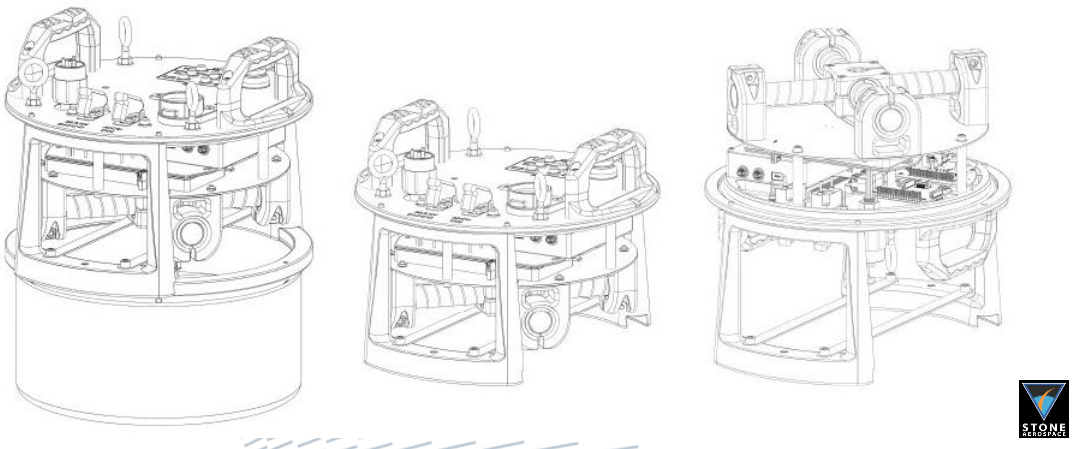

Figure 27: Diagram of the different possible uses of the Bench Jig assembly for puck serviceability

4.3 Component Highlights

4.3.1 Housing Manufacturing and Material Selection

The housing is the largest and costliest part in the puck assembly. Its role is critical, ensuring the functionality of the puck under both environmental and operating conditions. This subsection aims to delve into the trade-offs between machining and 3D printing as viable production methods for the part. Furthermore, it explores potential materials suitable for this purpose. The following trade-off analyses for the chosen process and material shed light on the complexities and considerations in the housing design and production.

Table 4: Trade-off analysis of puck Housing manufacturing process

	Machining	3D Printing
Cost	Raw material block: Acetal, Delrin ~$1,000 UHMW ~$1,500 Processing cost: > $1,000	$1,500 - $2,500
Weight	~3 kg, due to difference in features	2.25 kg
Lead time	> 21 days	5 - 7 days
Possible Materials	Acetal, Delrin, UHMW, PEEK, ULTEM	ULTEM, PEEK, Nylon, ABS, PC
Post-processing	None needed, tight tolerances achieved through process	Needed: for O-ring surface and/or water sealing. Available: epoxy sealing, vapor smoothing, resin filling, post-machining.
Low temperature performance	Ensured	Ensured for ULTEM and PEEK. Other materials need testing.
Material utilization	Very low, <10%	FDM and SLA: very high, depending on supports. SLS: high, depending on machine refresh rate.

Regarding cost, 3D printing and machining are quite similar. However, 3D printing has an advantage in lead time and results in a lighter component. It is essential to note that depending on the chosen material and the specific 3D printing technique, additional post-processing for water sealing and preparing O-ring surfaces may be necessary. When it comes to material utilization, 3D printing is more efficient, producing less waste which not only leads to cost savings but is also more environmentally friendly. With these considerations in mind, a comparison of various 3D printing materials was undertaken.

Table 5: Comparative matrix of commercially available 3D printing processes and materials. A red cell indicates a critical limitation, whereas a yellow cell denotes a point of concern

Process	Material	Vendor	Cost	Cold Temperature Performance	Water Absorption
MJF	Powdered Nylon, PA12	Vendor 1	$, $1,500	Undefined	Low absorption, 0.5%
SLA	ABS-Like	Vendor 1	$$$, $5,200	Undefined	Some absorption
SLA	PC-Like	Vendor 1	$$, $2,700	Undefined	Some absorption
HVP Extruder	PEEK	Vendor 2	$$$, $4,800	Excellent	Very low absorption, <0.1%
HVP Extruder	ULTEM AM9085F	Vendor 2	$$, $2,500	Excellent	Porous, needs sealing
FDM	ULTEM 1010	Vendor 3	$$, $2,100	Excellent	Porous, needs sealing
SLS	Nylon 12 CF	Vendor 3	$$$, $4,400	Undefined	Porous, needs sealing

Considering that the primary objective of the overall project is advancing the RF communication technology, it was decided to focus on materials already proven to perform well in cold temperatures rather than conducting extensive testing. Material strength was another vital factor in the selection process. Among the listed materials, PEEK stands out for its superior strength and excellent cold temperature performance; however, its steep cost made it impractical. ULTEM, which follows

closely in strength and has also demonstrated reliability in low temperatures, stood out as a viable choice. It is important to note that the substantial size of the housing, 30 cm in diameter and 15 cm in height, posed challenges not only in terms of size compatibility with available 3D printers but also in ensuring the proper curing of the part to avoid warping or the introduction of inhomogeneities.

Drawing insights from Table 4 and Table 5, the housing was fabricated using FDM 3D printing technology with ULTEM 1010 material. This choice was driven by ULTEM's established resistance to cold temperatures, superior strength, and cost compatibility with the budget. However, this combination requires post-processing, which included epoxy sealing to achieve watertightness and surface treatment for the O-ring interface.

4.3.2 O-ring Seal

The challenge with this particular O-ring seal is that it goes in between two parts that are made of two different materials and made by two different manufacturing processes. The housing is 3D printed ULTEM, while the lid is machined aluminum, meaning that the two parts have different values for coefficient of thermal expansion and different manufacturing tolerances.

Initially, the O-ring design chosen was the radial seal, where a designed gap exists between the moving components. This design would require a tight tolerance of about +/- .001” of the housing inner diameter to achieve the proper O-ring squeeze. These tolerances are hard to achieve with standard 3D printing methods due to the inherent geometrical accuracy of the processes and warping as the printed parts are bigger.

The corner seal or crush seal is used where cost and ease of machining are important. The triangular recess is simpler than the radial groove and the tolerances can be loosened. However, this type of seal permanently deforms the O-ring, and thus the O-ring must be replaced every time the puck is opened.

The O-ring design chosen for the PARTI-Pucks prototype puck is the face seal with half dovetail groove. The face seal decouples the dimensional tolerances between the lid and the housing. The groove is CNC machined into the lid, which can easily achieve tolerances in the range of .001” and tighter. The O-ring makes contact with the top of the 3D printed housing, which should only achieve a flat surface and a surface roughness suitable for sealing. The half-dovetail groove is implemented so that the O-ring cannot fall out. It should be mentioned that half-dovetail grooves add complexity and cost to the machining process, so, in this case, the advantage of such a groove justifies the additional cost.

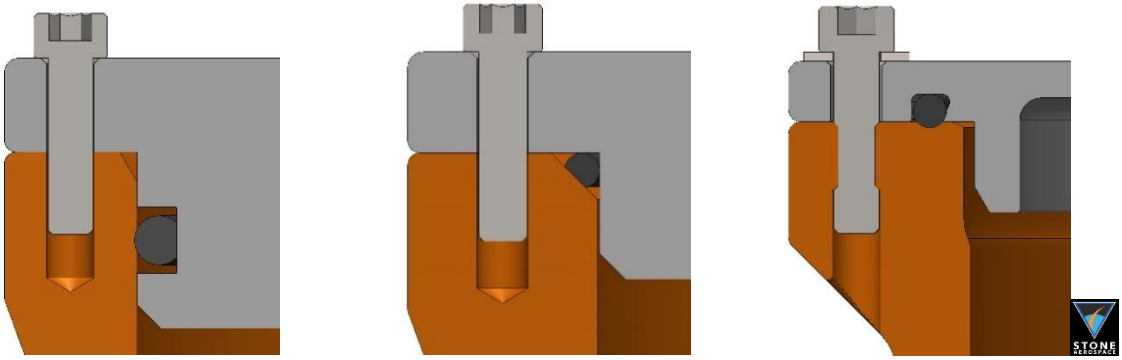

Initial O-ring Design: Radial Seal

Intermediate O-ring Design: Corner Seal

Final O-ring Design: Face Seal

Figure 28: Progressive design changes of the O-ring seal between the lid and the housing
Components: lid in grey, housing in orange and O-ring in black

For achieving a sealing surface on the 3D printed housing, a set of submersion tests were performed with three different surface variations:

1) Circular pattern on sealing surface, standard finish as-printed: according to the Parker O-ring guidelines, if the sealing surface is produced by turning the part on a lathe, or by some other method that produces scratches and ridges that follow the direction of the groove, a very rough surface will still seal effectively.

2) Circular pattern on sealing surface and epoxy sealant: the printed ULTEM is a slightly porous material, and thus epoxy sealant is used on all exposed surfaces to avoid any water absorption through the enclosure material.

3) Standard printed pattern, epoxy sealant, and filler on sealing surface: additional to the epoxy sealant on all surfaces, the sealing surface is heavily sanded and coated with a filler to achieve a lower surface roughness. However, the hand sanding operation may affect the surface flatness.

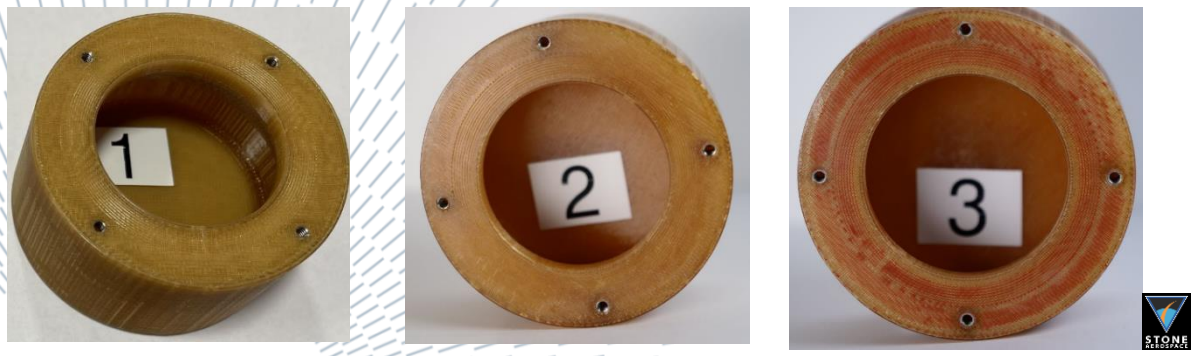

Figure 29: Picture of the three 3D printed housing variations for submersion tests, with different O-ring surface variations

The small-scale lid and housing assemblies were sealed with a water leak test paper inside. The assembly was weighted before and after a one-hour shallow water submersion and the leak test paper checked for any signs of moisture inside the enclosure. In this way, both leaking inside the enclosure through the O-ring seal and water absorbed through the printed enclosure were being monitored. Test sample #1 with no epoxy sealing failed the test, while both test samples #2 and #3 passed the test.

Surface variation #2 has a lower manufacturing cost and a higher repeatability at larger scales than surface variation #3 since it does not involve hand sanding. A circular pattern on sealing surface and epoxy sealant on all surfaces ensures a roughness and flatness suitable for the O-ring design, which is why we chose surface variation #2 for the housing design.

4.3.3 EMI Enclosures

One of the requirements set forth by the Radio Frequency team entailed the construction of Electromagnetic Interference (EMI) shielding around the HackRF One board, which functions as the Software Defined Radio (SDR) transceiver of the system, along with the HF and UHF circuits present on the FAM board. The principal objective was to create a conductive enclosure akin to a Faraday cage, with connection points at intervals of 1 cm (0.4 in) or less for any apertures, in accordance with the signal frequency. Additionally, the design needed to facilitate repeated assembly and disassembly to accommodate maintenance and diagnostics.

A prevalent method for EMI shielding involves employing bent metal enclosures that are fixed via tack soldering. Nonetheless, this technique is permanent, which rendered it incompatible with the project's requirements. An alternative method encompasses the use of a four-sided base that is soldered into position, coupled with a lid with snap-fit mechanisms and incorporates features ensuring contact at predetermined intervals. Although bent metal enclosures are frequently employed in industrial designs for large-scale production, this approach becomes unfeasible for smaller batches. Consequently, the decision was made to adopt a strategy involving the 3D printing of enclosures followed by coating them with conductive nickel paint, a proven, cost-effective technique previously employed at Stone Aerospace.

Given that the HackRF One was designated to be assembled to the lid, it was possible to incorporate features into the lid design that would accommodate the EMI enclosure. This enclosure was devised with tabs spaced less than 1 cm apart and an interference fit with the puck lid of approximately 0.13 mm (0.005 inches), thereby ensuring contact through pressure. Six screws serve to secure the enclosure and

concurrently function as contact points. To further improve the EMI shielding, a gasket made of polyurethane foam covered in conductive nickel is adhered to the edge of the lid using conductive adhesive, filling any possible gaps between the shield and the lid.

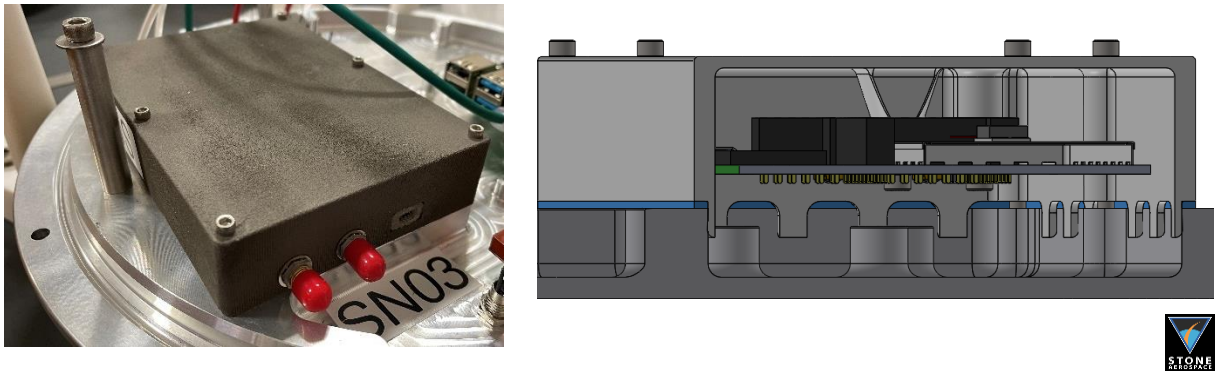

Figure 30: HackRF One EMI Shield. On the left, picture of the shield assembled to the lid. On the right, section view of the model, showing the tabs making contact with the lid and the EMI gasket shown in blue

For the HF and UHF circuits, an alternative strategy was required. These circuits on FAM board limit the incorporation of machined fastening features. The chosen approach involved using a soldered base coupled with a removable lid, utilizing a machined brass base and a 3D printed lid coated with nickel conductive paint, similar to the HackRF shield. Given the absence of fasteners to secure the lid, a meticulous analysis was necessary to design snap-fit features that would effectively hold the lid in position.

Calculations were conducted based on the deflection at the free end of a beam, and the geometry underwent multiple iterations, considering the mechanical properties of the Nylon PA12 material and standard design ratios for snap fits. The objective of this analysis was to achieve a total insertion force not exceeding 40 N, with a total separation force ranging between 40 and 50 N. The preliminary calculations were based on full contact between the base and the lid, disregarding the effects of the EMI gasket in between. The flexible material gave the assembly slack, resulting in low insertion and separation forces of the initial set of prototypes. The finalized design was obtained by adjusting the geometry to increase the forces by approximately 25%, and this design proved successful.

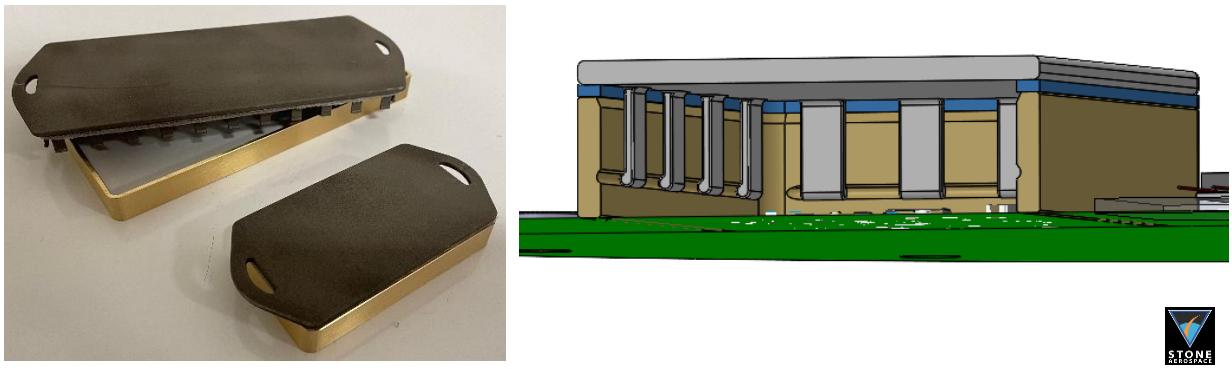

Figure 31: HF and UHF circuits EMI Shields. On the left, picture of the shields to be installed on the FAM board. On the right, section view of the UHF model, showing the tabs, the snap fit groove on the brass base and the EMI gasket shown in blue

4.3.4 User Interface

In the challenging environment of a Moulin, where operators will encounter low light, freezing temperatures, and potentially precarious positions such as being suspended from ropes against icy walls without a stable footing, the design of the puck's user interface demands careful consideration. It is critical that the user interface be effortless to navigate and interact with under these harsh conditions. Top priorities include accommodating the use of heavy winter gloves, providing robust rigging points, ensuring the ease of connecting and switching components, and incorporating intuitive status indicators.

UI Initial Design UI Intermediate Design UI Final Design

Figure 32: Progressive design changes of the User Interface components and locations on the prototype puck lid

The evolution of the user interface design can be observed through three distinct stages, depicted in Figure 32. The initial design featured a plastic lid, with LEDs uniformly spaced on the top half of the lid, connectors and switches on the bottom half, two simple off-the-shelf handles, and a groove feature integrated across the lid for a strap or cord, enabling the puck to be pressed firmly against the glacier ice for a sustained contact between the patch antenna and the ice.

As the design progressed, it became apparent that an aluminum lid was necessary for effectively dissipating the internal heat. Moreover, as electronic components began to be mounted on the inner side of the lid, this led to a reconfiguration of the LEDs to be positioned closer together. An additional safety feature was added in the form of an emergency switch, the Main Disconnect switch, that enables immediate power cut-off in the event of any issues during testing.

In the final design, further refinements were made. The LEDs on the top were clustered towards the center, while those on the bottom were repositioned to the sides of the switches, optimizing space utilization. To improve visibility and association, all components related to power were chosen to be red. An extra mounting point was introduced for the Disto-X, and the data connector was relocated to the top, as it is used only for data retrieval and not during operation. This final layout ensures that during deployment, the top half of the puck is dedicated to indicators, while the bottom half comprises connectors and switches that require operator interaction. Additionally, the strap used to press the puck against the ice is designed to run across the puck, either above or below the handles, adapting to the ice profile encountered.

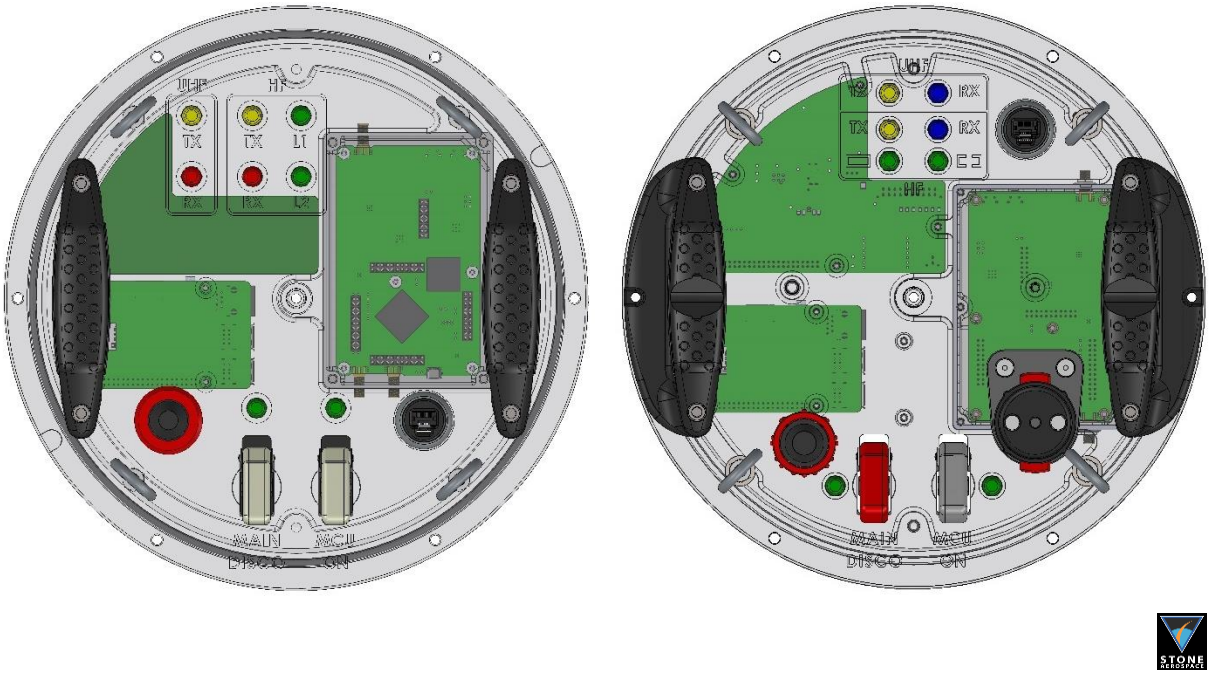

UI Intermediate Design UI Final Design

Figure 33: Comparison of the electronic boards and user interface component locations. The final design arrangement has an increased available footprint for the interface board on the top left and presents a more symmetric design

The improvement of the user interface, as depicted in Figure 33, was achieved through a systematic evaluation of the lid's features. Specifically, the features that penetrated through the lid, such as the through-holes for LEDs, switches, and connectors, were distinguished from those present on only one side of the lid, like the labels on the exterior and the bosses for the boards on the interior. Upon this differentiation, the features that were present on both sides were consolidated in a compact arrangement. For instance, the LEDs were assembled in a tight cluster at the top. This strategic arrangement facilitated the positioning of labels around the LED holes on the exterior, while simultaneously allowing for the boards to occupy the corresponding space on the opposite side of the lid. This methodical organization not only improved the available space but also enhanced the overall functionality and usability of the interface.

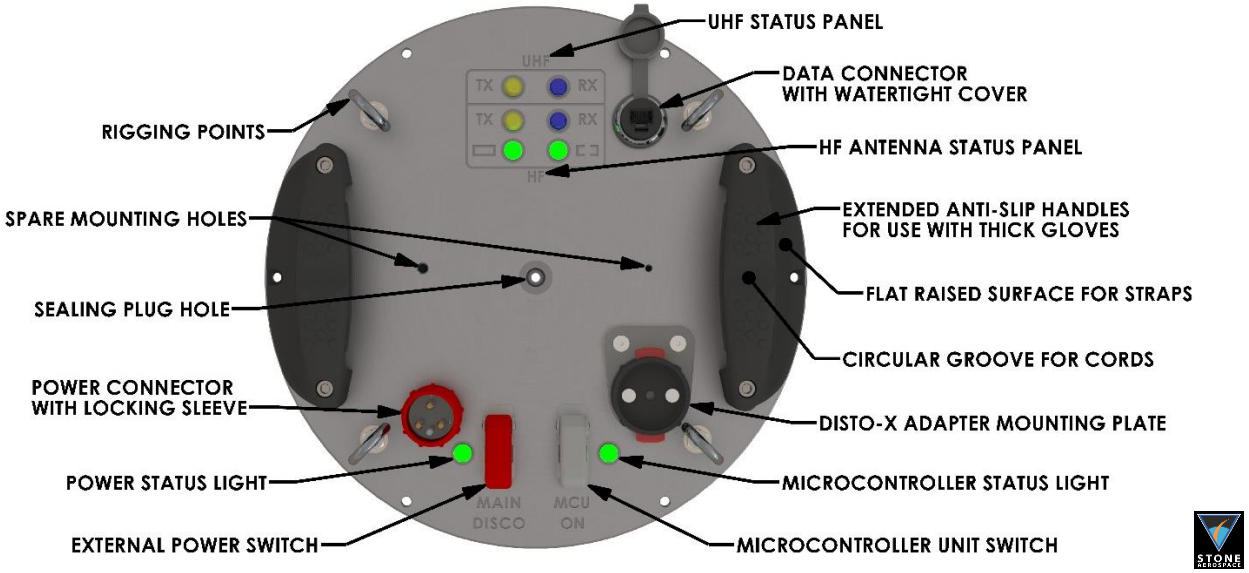

Figure 34: Puck User Interface diagram with labeled features

The status lights and switches are accompanied by short abbreviations or symbols explained in the following table.

Table 6: Reference table of the User Interface indicator light labels and their meaning

Indicator Light Label	Color	Meaning when light is ON
UHF – TX	Yellow	UHF Patch Antenna is transmitting
UHF – RX	Blue	UHF Patch Antenna is receiving
HF – TX	Yellow	HF Crossed-Loop Antenna is transmitting
HF – RX	Blue	HF Crossed-Loop Antenna is receiving
HF – ▭	Green	HF Crossed-Loop Antenna solid loop is tuned
HF – [ ]	Green	HF Crossed-Loop Antenna split loop is tuned
MAIN DISCO	Green	Main Power Disconnect. External power source is connected and on. Toggle switch to OFF position in case of emergency or during transportation.
MCU ON	Green	Microcontroller Unit is on. Toggle switch to OFF position to reset.

Figure 34 and The status lights and switches are accompanied by short abbreviations or symbols explained in the following table.

Table 6 serve as portable reference guides for the team in the deployment site to efficiently familiarize themselves with the puck's user interface features and quickly interpret the meanings of the indicator light labels. This preparatory measure is aimed at facilitating smoother operation and improving the effectiveness of the team in handling the pucks under the demanding conditions of the field.

4.4 Overall Costs

The cost of the PARTI-Pucks prototypes can be divided into three main categories: design development, hardware, and assembly costs.

The first category, design development, encompasses a wide range of activities, including but not limited to, system architecture, antenna design and testing, custom board development, and many other facets in addition to the mechanical design. Overall, the design process spanned approximately a year and a half, stretching from the initial project launch to the culmination in the final design. The design development cost was monitored at the project level, thus it becomes challenging to isolate and quantify the expenditure specifically associated with mechanical design and development. However, an important consideration during the design development phase was the cost-effectiveness of certain choices. For this development stage, it was critical to recognize the point at which a component reached an adequate level of development, even if it was not optimized in terms of weight or cost, as any further time invested in improvement could escalate the overall development expenses.

In terms of hardware costs, it is worth noting that the Lid and Housing combined account for over half of the total hardware expenditure for the puck. These components are not only the most sizable, but also have a critical role in ensuring optimal performance in varying operational and environmental conditions.

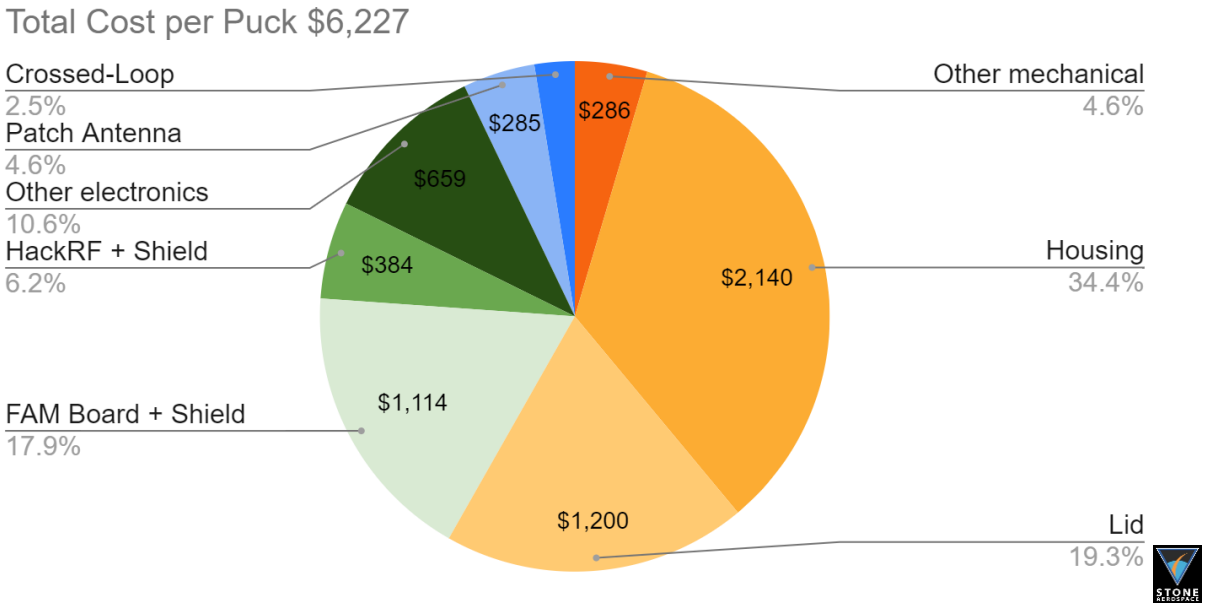

Figure 35: Pie chart of the hardware cost breakdown for a prototype puck, color-coded in different shades by categories: mechanical components in orange, electronics components in green, and RF antennas in blue

The total hardware cost for the construction of four pucks is approximately $25,000. A pair of pucks is required for a successful execution of tests, while the additional two serve as redundancy, ensuring the continuity of testing in the unforeseen event of component failure in the field.

Regarding the assembly costs, the mechanical integration of components was completed by two engineers, within a span of one week. With an hourly rate estimated at $50, the mechanical assembly cost is around $4,000. Similarly, the integration of electronics and wiring, which is anticipated to take an equivalent duration of one week with the involvement of two engineers, adds an approximate $4,000, summing a total of $8,000 for the complete assembly of the four pucks.

At the time of writing this thesis, mechanical integration has been completed, while final integration is in the plans.

Additional costs such as those associated with field deployment fall beyond the scope of this analysis. Notwithstanding, a conscious effort was made to reduce design, hardware, and assembly costs, to ensure a more flexible financial allocation for field deployment activities.

5 Analyses and Results

5.1 Structural Analyses

In this section, we delve into the assessment of specific components of the prototype puck that are subjected to forces which could potentially lead to failure. It is critical to note that while the prototype puck does not encounter extraordinary forces, there are components, namely the housing and the FAM board, which demand careful evaluation. The housing experiences compressive forces when attached against the glacier walls. The FAM board, constrained by the commercially available thicknesses of electrical boards, bears the load due to the weight of the crossed-loop antenna assembly.

Finite Element Analysis, through SOLIDWORKS Simulation, was employed to critically assess these components. The primary objective of these analyses is to verify that the design is robust enough to prevent any functional issues, as opposed to striving for weight reduction or optimization. It is essential to bear in mind that the puck in consideration is a prototype and not flight-ready hardware; hence, a component that fulfills its purpose in a sensible manner is favored over an optimized component achieved through a significant amount of development time.

5.1.1 Housing

To calculate the compressive force that the housing undergoes while making contact with the glacier ice, it is important to first comprehend the method by which the puck is affixed to the ice. Initial tests were conducted by the lead of field deployment in an environment that closely mimics the icy conditions of a glacier. The procedure involves the installation of ice screws at strategic points. Two screws are placed laterally to suspend the puck at the desired height using the eyebolts on the lid, while two more screws, aligned with the puck's central axis, are employed to exert pressure against the ice through the handles. The latter pair of ice screws is equipped with straps and a bar that can be rotated. This rotation tightens the straps, functioning akin to a tourniquet, increasing the pressure exerted with each turn. Figure 36 depicts the tourniquet in a vertical orientation, though it is worth noting

that it can also be rigged horizontally, rotating the puck and the tensioned line by 90 degrees.

Figure 36: Puck to ice test, using a puck-analog in an icy environment, to test rigging procedures

The force required to maintain the puck bottom against the ice in a vertical wall is minimal, as the lines to the eyebolts are the ones holding the weight. The edge case is when the puck is installed on an overhanging wall, approaching the horizontal. In this case, the surface puck would be placed almost vertically above the moulin puck, decreasing the transmitting distance, so this is not a condition that is likely to occur in the field. However, this condition serves as a good estimate for the possible maximum force exerted on the puck housing.

In this edge case, the tourniquet strap would be applying a force on the handles equal to the puck weight, at 68.7 N (7 kilograms mass). This force is transferred to the lid, and through the housing, which is the object of study.

A simplified model was built, taking advantage of symmetry, to verify the performance of the housing under this load. The assembly model includes the housing, the patch antenna, and a simplified lid with the handle footprint for applying the force. Due to symmetry, the applied force is only half, at 34.3 N (3.5 kg mass).

The material properties of ULTEM 1010 are modeled after Stratasys' datasheet. Note that the ZX orientation, the vertical one as the part is printing, is exactly the direction

subjected to the compressive forces. However, for simplicity, the housing material is modeled as a linear elastic isotropic material, with the weakest orientation values as a conservative approach. Therefore the tensile strength at break is set to the ZX orientation value, while the compression yield strength is set to the lower XZ orientation value. It is worth noting that the standard deviations of the strength values are significant, for example the ZX strength at break is 28.2 MPa, while the standard deviation is 8.8, over 30% of the value.

		XZ Orientation[1]	ZX Orientation[1]
Tensile Properties: ASTM D638			
Yield Strength	MPa	No yield	No yield
	psi		
Elongation @ Yield	%	No yield	No yield
Strength @ Break	MPa	79.2 (4.9)	28.2 (8.8)
	psi	11500 (710)	4080 (1300)
Elongation @ Break	%	4.0 (0.42)	1.1 (0.45)
Modulus (Elastic)	GPa	3.04 (0.18)	3.00 (0.45)
	ksi	441 (27)	435 (65)
Compression Properties: ASTM D695			
Yield Strength	MPa	245 (50)	438 (31)
	psi	35600 (7200)	63500 (4500)
Modulus	GPa	2.93 (0.14)	3.23 (0.57)
	ksi	425 (20)	468 (83)

[1] Values in parentheses are standard deviations.

Figure 37: ULTEM 1010 mechanical properties, as reported by Stratasys

In this preliminary assessment, an initial FEM study was conducted considering the variability in material properties. To this end, the minimum orientation value was decreased by three times the standard deviation to determine the yield strength in tension (1.8 MPa) and compression (95 MPa), thereby considering the lower extreme of the distribution. It is worth highlighting that this method is employed in critical engineering applications and is typically accompanied by an evaluation of the upper extreme of the force application distribution. Employing such a conservative approach initially contributes to identify potential issues in the design.

The assembly model under analysis comprises a 7.6 mm (0.3 in) thick ULTEM housing, a simplified aluminum lid, and a G10 Fiberglass patch antenna. By leveraging symmetry, constraints are applied to the bottom surface of the housing and patch antenna, setting vertical displacements to zero, and lateral movements are restrained by fixing a small central area on the patch. The load of 34.3 N is applied across the surfaces representing the handle interface on the lid.

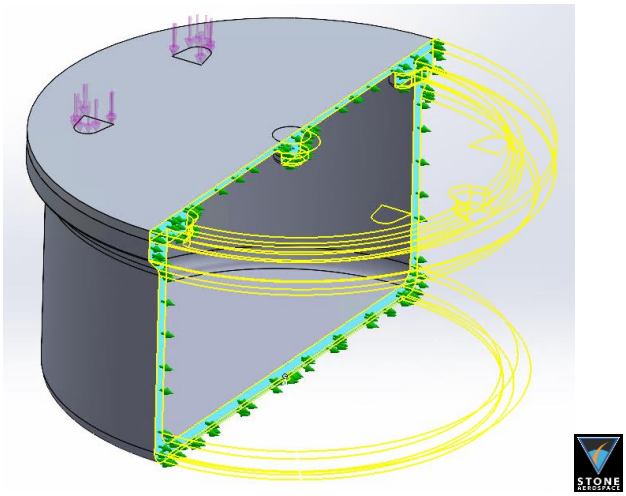

Figure 38: Housing finite element analysis constraints and loading conditions

In terms of solid mesh control, the housing elements are configured with a size of 2 mm and a ratio of 1.4, whereas the lid and patch antenna are designed to accommodate at least two elements across their thickness.

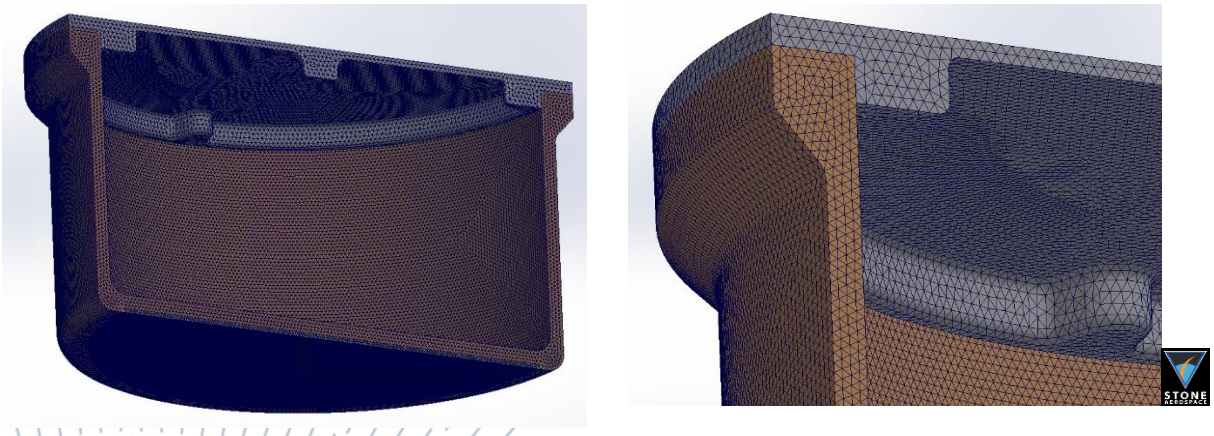

Figure 39: Housing finite element analysis mesh

The analysis reveals a peak stress of 1.2 MPa, which is localized at a corner of the lid. In contrast, the stress experienced by the housing is significantly lower, by an order of magnitude. Deflections are similarly marginal, with a maximum displacement of 0.007 mm at the center of the lid, and the housing exhibits virtually no deflection.

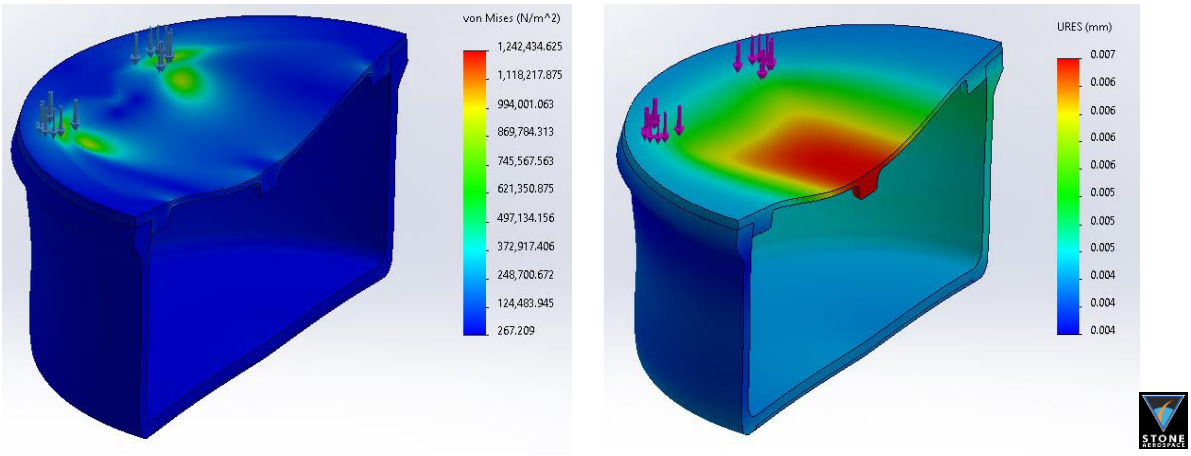

Figure 40: Housing finite element analysis, resulting stress and deflection plots of initial study, with a 34.3 N force applied

These results, characterized by low stress levels and minimal deflection, both in the housing and the lid, affirm that the anticipated loads on the puck do not pose any concerns, eliminating the need for further refinement in the analysis. Moreover, even if the tourniquet strap were to apply a force 2 or 3 times the puck's weight, the structural integrity would not be compromised.

Taking into consideration these findings, should this prototype puck design be adapted for an actual mission-ready application, the implications of such a low-stress and deflection profile would lead to a subsequent phase of topological optimization aimed at minimizing volume and weight, enhancing efficiency and performance.

5.1.2 FAM Board

The Finite Element Analysis (FEA) of the FAM Board, loaded by the weight of the crossed-loop antenna assembly, served two objectives: first, to ensure that the board would not sustain damage due to excessive stress or deformation, and second, to inform the optimal placement of connectors on the board by identifying areas with minimal deflection.

The assembly model for the analysis comprised the FAM board, simplified representations of the HF and UHF EMI boxes as extruded bosses, a simplified central standoff and side standoffs for the crossed-loop, and a weld bead pattern surrounding both boxes. The board was modeled as a standard electrical board thickness of 1.6 mm, while the 3mm-diameter weld beads were positioned at 1 cm intervals. For simplification, the crossed-loop antenna was excluded from the model, with its weight being represented as a load directly exerted upon the standoffs.

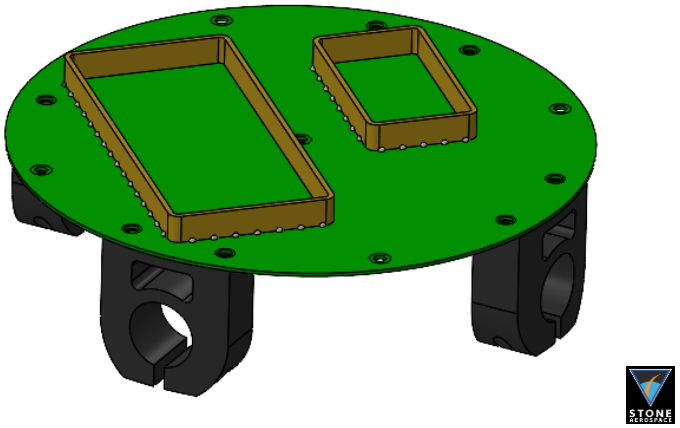

Figure 41: FAM Board finite element analysis assembly model

G10 fiberglass was selected as the material for modeling the FAM board, given that electrical boards typically employ FR4, a flame-retardant variant of G10.

Table 7: FAM Board structural analysis assembly components, materials and yield strengths

Component	Material	Yield Strength [MPa]
FAM Board	G10 Fiberglass	262
Center Standoff	Nylon PA12	53
Side Standoff	Nylon PA12	53
HF Box	Brass	338
UHF Box	Brass	338
Weld Bead	Tin-Silver Solder	36

In terms of constraints, the surfaces where the board is fastened to the lid (in contact with the spacers) were designated as fixed. The load was configured as a distributed remote load, centered at the antenna's center of mass, and coupled to the standoff surfaces interfacing with the crossed-loop antenna. The load was computed as a shock load, equivalent to four times the crossed-loop's weight, totaling 4.88 kilograms. The load direction was a variable parameter in the different studies.

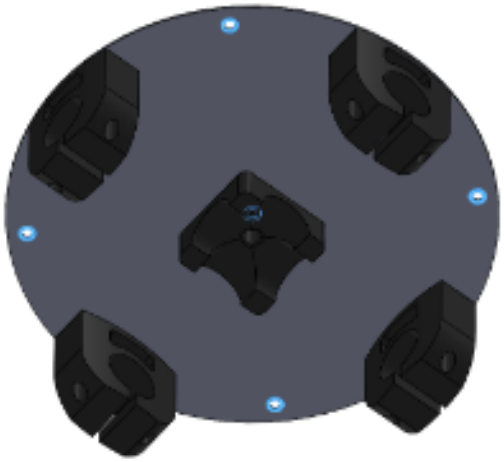

Figure 42: FAM Board structural analysis constraints, fixed surfaces shown in blue

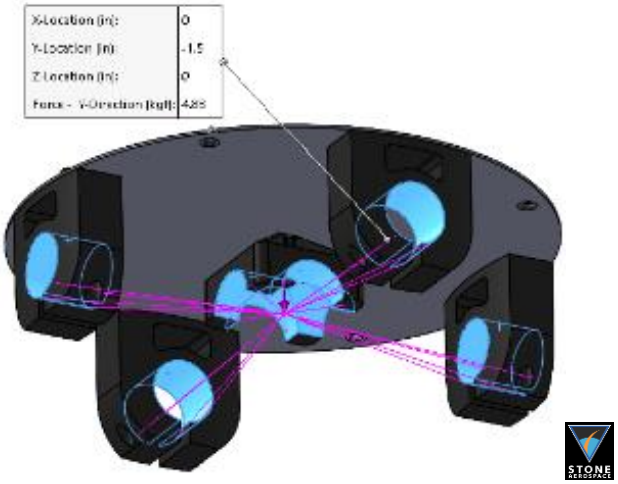

Figure 43: FAM Board structural analysis loading, remote load applied on blue surfaces at the pink arrow location

The mesh employed was a high-quality solid mesh with an element size of 7.6 mm and a tolerance of 0.38 mm. Moreover, the FAM board incorporated mesh control with a 1.5 mm size and a 1.4 element ratio. The component interactions were globally set as bonded, with contact interaction assigned between the FAM board and the HF and UHF boxes.

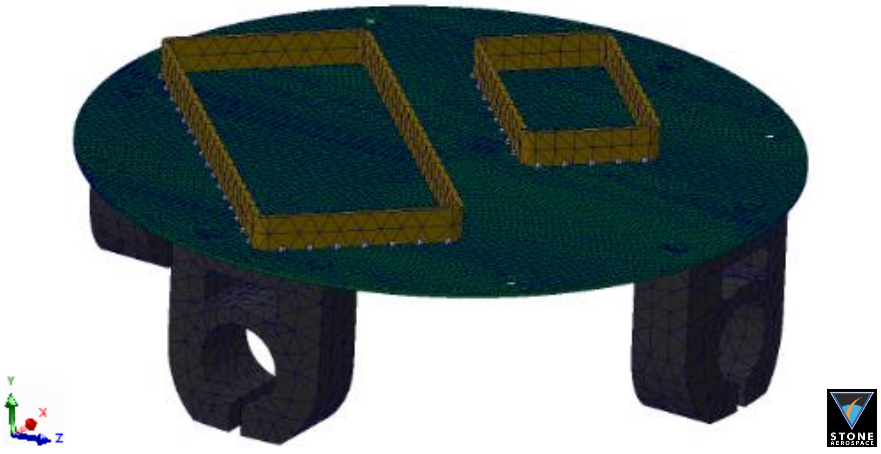

Figure 44: FAM Board structural analysis mesh

Multiple studies were performed, with load directions including vertically downward and at 45 degrees from the horizontal in different orientations.

Table 8: Summary table of FAM Board structural analysis study results, given a load direction

Study #	Input				Output	
	Load direction	X Load value [kgf]	Y Load value [kgf]	Z Load value [kgf]	Max. Stress [Mpa]	Max Board Deflection [mm]
FAM-ASSY-1	-Y	0	-4.88	0	72.3	0.58
FAM-ASSY-2	45deg -Y+Z	0	-3.45	3.45	50.8	0.25
FAM-ASSY-3	45deg -Y+X	3.45	-3.45	0	50.9	0.48
FAM-ASSY-4	45deg -Y-Z	0	-3.45	-3.45	50.8	0.84
FAM-ASSY-5	45deg -Y-X	-3.45	-3.45	0	50.7	0.46

The first study revealed a maximum stress of 72.3 MPa. Considering the substantial margin between this figure and the yield strength of G10 at 262 MPa, stress is not deemed a concern. However, deflections were significant. Evaluating the deflection plots, the maximum deflection occurs along the board's edge, away from electrical connections and circuits.

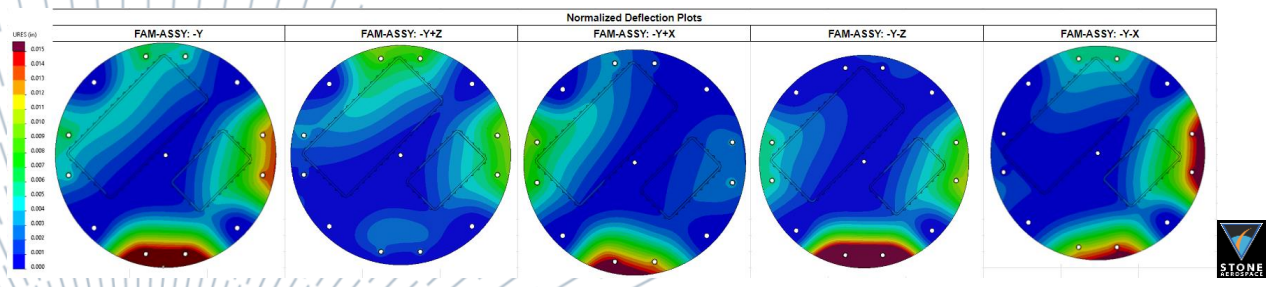

Figure 45: FAM Board structural analysis deflection plots, normalized to .015 in (0.38 mm) and displaying 15 color gradients, so every color change represents a .001-in step

Figure 45's deflection plots were visually inspected to define the regions with the least deflection gradients. Lesser deflection gradients imply regions where color transitions in the plot are more spaced out.

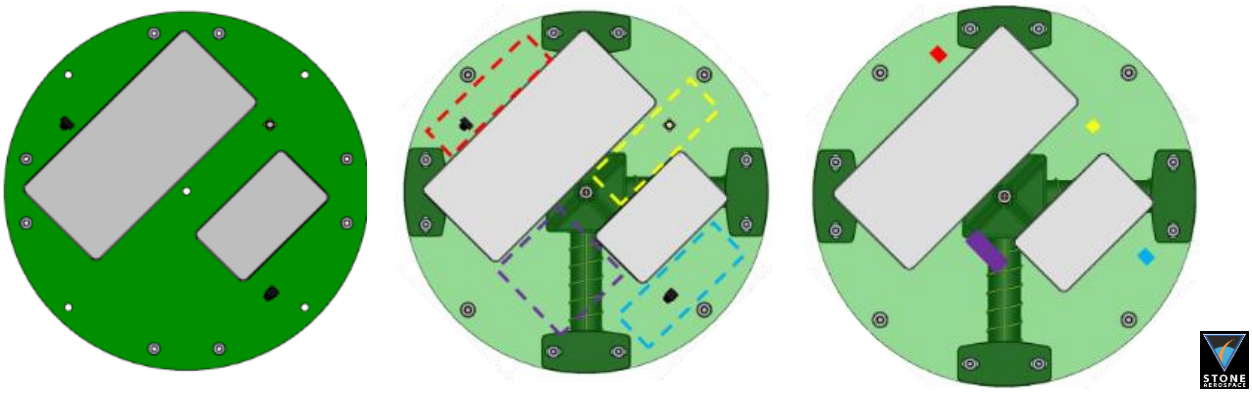

Initial Design **Position Bounds** **Final Design**

Figure 46: FAM Board connector location analysis, based on structural analysis deflection plots

Following the analysis, which validated the connector placements and confirmed the absence of critical stress levels, it was still emphasized that precaution must be exercised to avoid dropping the puck.

5.2 Thermal Analyses

A crucial aspect of the puck assembly design lies in the effective thermal management, particularly given that the device operates within a cold environment and a significant portion of the battery's power input is expended as heat between the crossed-loop antenna and the electronics within the puck.

There is a delicate balance to be maintained in thermal management. On one hand, there is a risk of excess heat being trapped within the enclosure due to inadequate dissipation to the surrounding environment, which could cause the internal electronics to overheat, potentially reaching temperatures of 60-70°C. Conversely, if an excessive amount of heat is dissipated into the cold surroundings, the internal temperature of the puck could go below 0°C, which is the lower threshold for the operation of the Commercial Off-The-Shelf (COTS) boards. Moreover, it is critical for the puck to maintain a temperature above freezing in order to be switched on and to start operations.

As the temperatures within the Moulin have not been extensively researched, environmental conditions have been estimated based on data gathered from previous Moulin field expeditions and analogous environments. The ice within the Moulin at the time of year schedule for testing is approximated to have a

temperature range of -15 to -5°C, whereas the air within the Moulin could be lower, between -30 and -5°C.

To analyze these thermal aspects, SOLIDWORKS Flow Simulation was employed. This tool, which is based on Computational Fluid Dynamics (CFD), utilizes the finite volume method to simulate and analyze the thermal dynamics within the puck assembly. Such analyses are essential in ensuring the reliability and functionality of the puck's electronics under the challenging thermal conditions of the operating environment.

5.2.1 Preliminary Thermal Analysis

Three crucial system components need to be maintained above freezing temperatures for the system to operate reliably: the HackRF One, enclosed in a dedicated nickel-coated plastic EMI enclosure; the FAM board, housing the HF and UHF circuits within brass and plastic EMI enclosures; and the Raspberry Pi.

In the initial prototype design of the puck, electronic boards were mounted onto the FAM board, clustering the electronics area as a separate module. As depicted in Figure 47, the FAM board functioned as a mounting platform for the HackRF Ones - initially designed with two boards within an EMI enclosure - along with the Raspberry Pi, and the FAM board circuit which is contained in the white EMI enclosure visible on the left side.

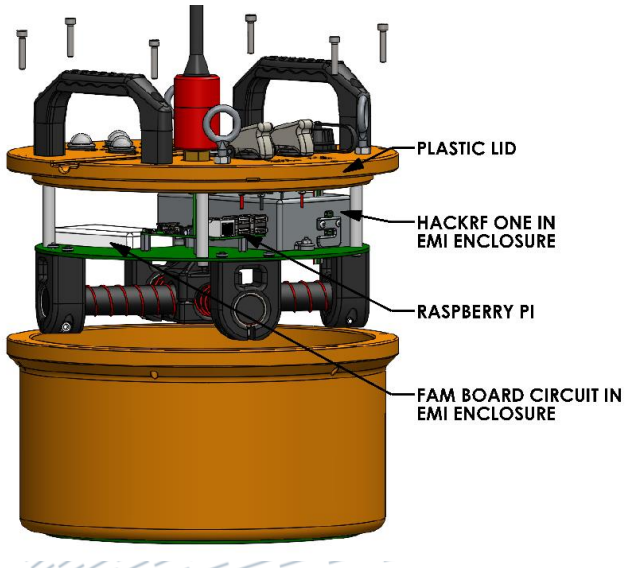

Figure 47: Exploded view of the initial prototype puck design, with the electronic boards mounted to the FAM board

A thermal model was constructed to simulate the temperature profile inside the puck, considering the heat generated by the boards and the influence of external environmental conditions on the puck. The specifics of the setup are elaborated in the following subsection.

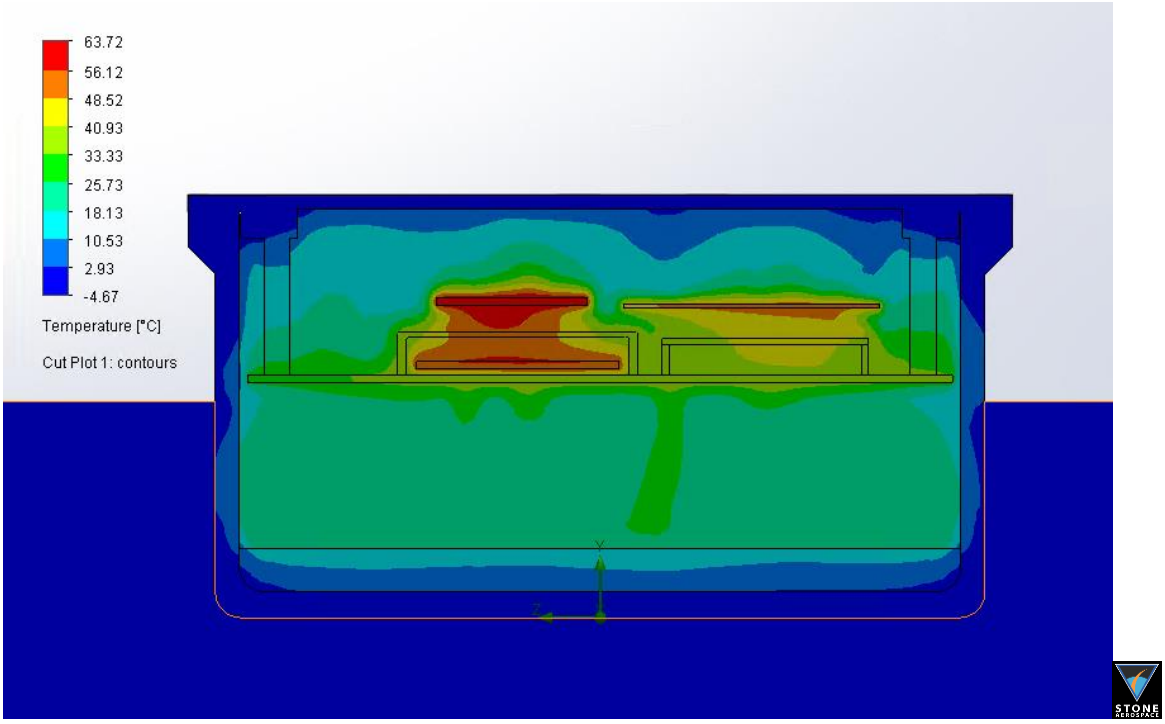

Figure 48: Puck preliminary thermal model results, performed on an assembly with electronics mounted on the FAM board

The results from this design, where electronics were clustered towards the center of the puck sealed with a plastic lid, showed temperatures exceeding 60°C, raising concerns about overheating. Consequently, the decision was made to relocate all PCBs, except for the FAM board due to its size, towards the lid, and to switch the lid material to aluminum with a higher heat transfer coefficient. This change aims to enable better heat dissipation to the surroundings and regulate the internal temperature more effectively.

5.2.2 Complete Thermal Analysis

The model incorporates a simplified geometry for the components mentioned in Table 9. It focuses on the electronics and excludes antennas and user interface components for simplicity. Ice is represented as a 60-centimeter solid mass, sufficiently large to simulate an expansive ice wall that remains undisturbed by the puck's thermal effects. Cold Moulin air is represented through a boundary condition.

The thermal model accounts for heat conduction in solids, the influence of gravity on natural convection which drives air mixing inside the puck, and includes both laminar and turbulent flow types. Radiation and humidity effects are omitted, and time dependency is disabled as it is not essential for determining steady-state conditions.

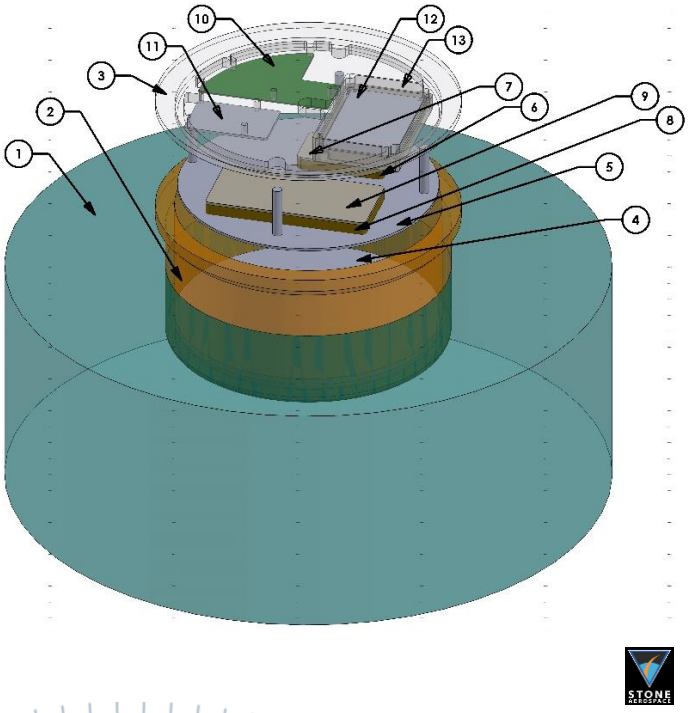

Figure 49: Puck Thermal Model Components

Table 9: Puck Thermal Model components and materials

	Component	Material
1	Ice	Ice -10C
2	Enclosure	ULTEM 1000
3	Lid	Aluminum
4	Foam	Polyurethane foam
5	FAM board	PCB 4-layers
6	UHF box base	Brass
7	UHF box lid	ULTEM 1000
8	HF box base	Brass
9	HF box lid	ULTEM 1000
10	Interface board	PCB 4-layers
11	Raspberry Pi	PCB 4-layers
12	HackRF	PCB 4-layers
13	HackRF EMI box	ULTEM 1000

The computational domain envelops all components, with four fluid subdomains filled with air: the main cavity of the puck, the interior of the HackRF EMI enclosure, and the two spaces beneath the FAM EMI enclosures. These fluid subdomains are assigned zero-velocity flow parameters, with both laminar and turbulent flow types. All fluids and solids have initial conditions set at -5°C, to assess potential overheating in scenarios involving the warmest ice and air conditions estimated for the Moulin, assuming the puck has reached ambient temperature during descent.

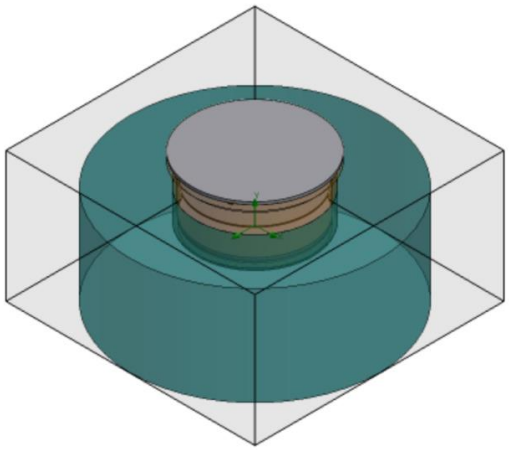

Figure 50: Puck thermal model, computational domain

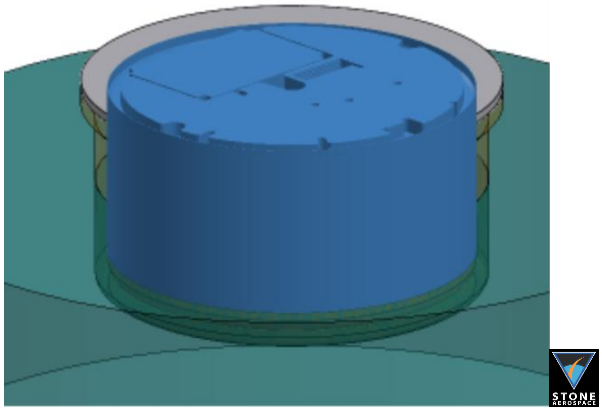

Figure 51: Puck thermal model, main fluid subdomain in blue

Ice and air cooling effects on the puck are represented as boundary conditions. The ice exterior is set at -5°C with no heat transfer, while air is modeled as an exterior boundary at -5°C with a heat transfer coefficient of 25 W/m2K, approximating air at very low velocities (around 2.5 m/s).

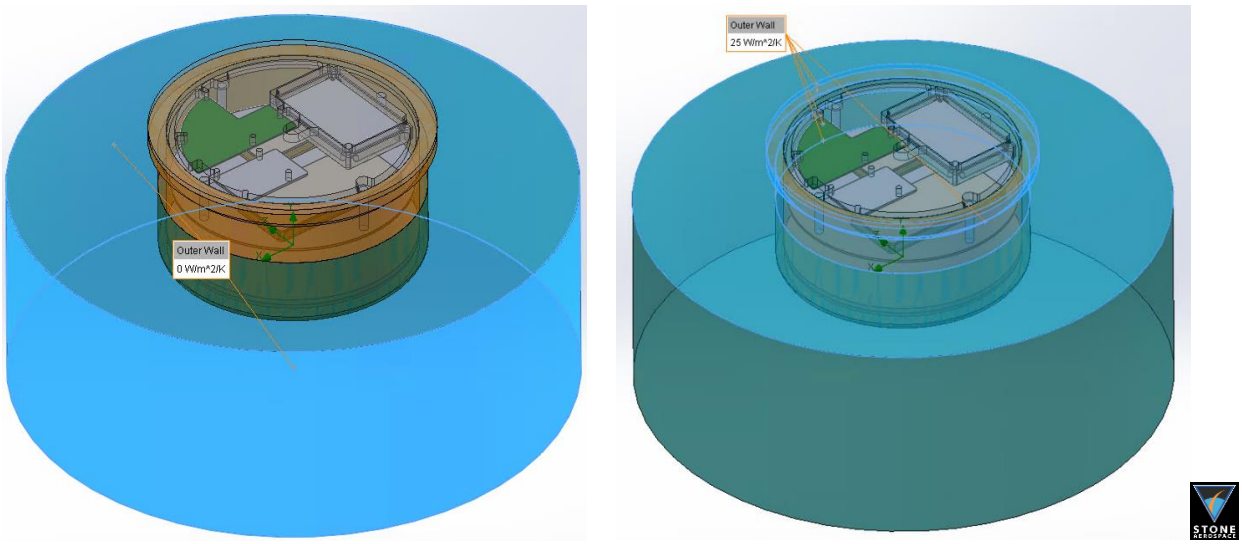

Figure 52: Puck thermal model boundary conditions. BC-ice on the left, outer wall with no heat transfer, and -5°C. BC-air on the right, outer wall with 25 W/m²K heat transfer coefficient at -5°C

Heat sources are simulated as a surface heat generation rate on the side of the board housing the components. This rate is derived from calculations by the electronics and RF team based on system heat dissipation. A more precise but computationally demanding model would pinpoint specific board components as heat sources.

However, for estimating steady-state conditions, a heat generation rate from a broader surface is a good representation.

Table 10: Puck thermal model heat sources, as heat generation rates for each board component

Component	Heat generation rate [W]
HackRF	2.67
Raspberry Pi	2.67
Interface Board	3.14
HF Board	2.54
UHF Board	2.86

The mesh is configured with a result resolution level of 5, without narrow channel refinement. In terms of geometry resolution, both minimum gap size and minimum wall thickness evaluations are automated. This yields a mesh with sufficiently fine fluid elements, and more refined solid elements for thin boards and solid-fluid interfaces.

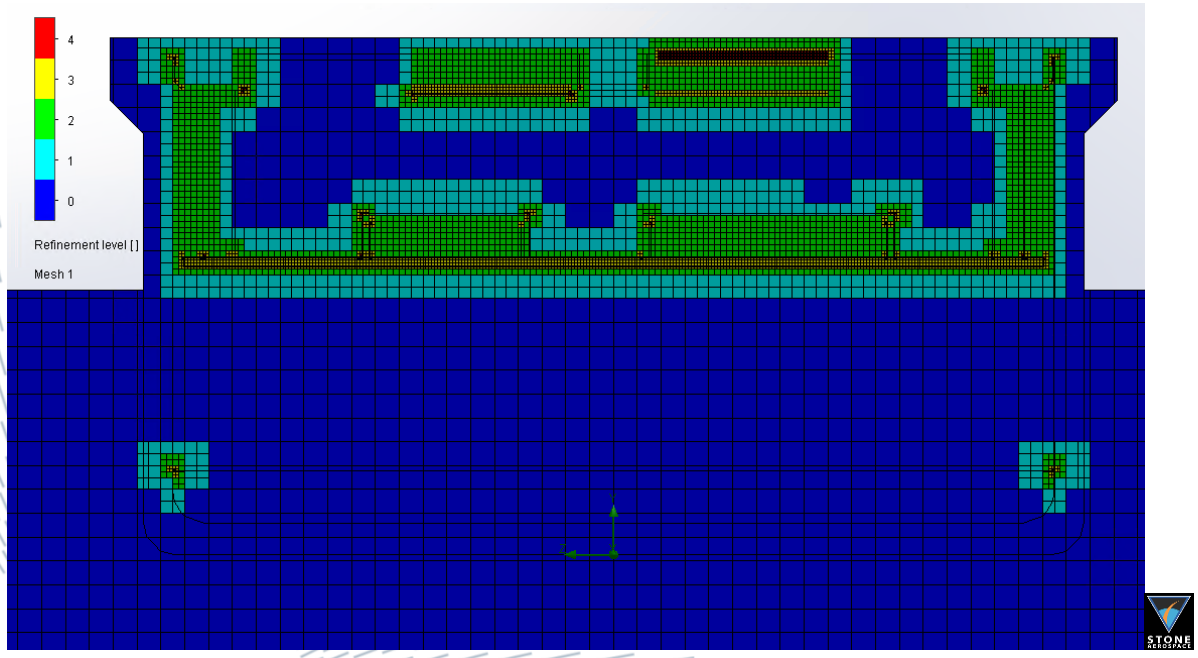

Figure 53: Puck thermal model, mesh refinement level plot

The study's results depict a temperature profile below the maximum of 60°C, with a maximum of only 35°C. The air exhibits a much-improved gradient inside the puck. The insulating polyurethane foam at the base of the puck housing demonstrates its efficacy as a thermal barrier, with a significant temperature difference between the component and the adjacent fluid.

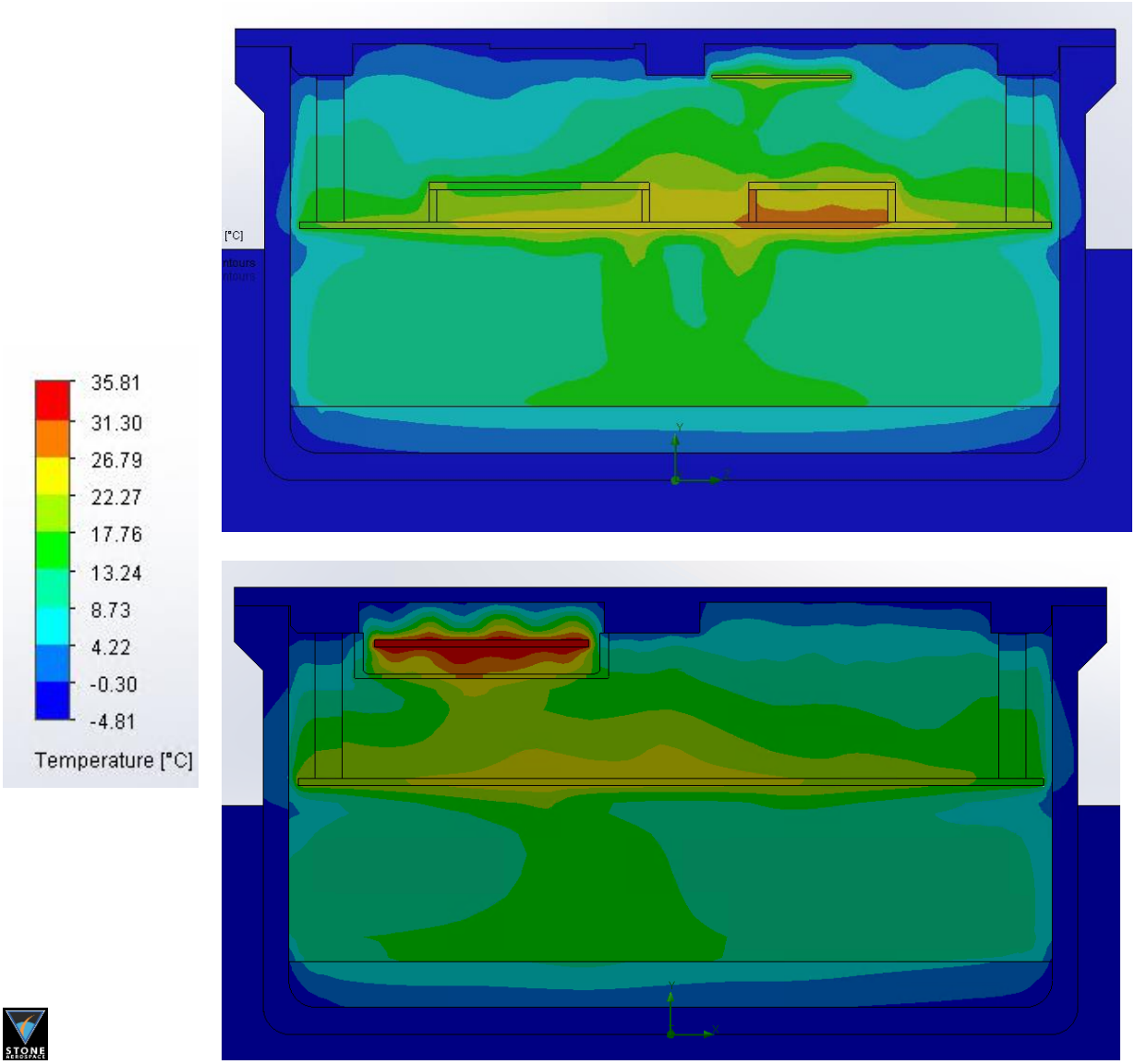

Figure 54: Puck thermal model, temperature plot of the ZY (above) and XY (below) section views of the model

Although the aluminum lid does not exhibit a temperature gradient, this model was compared to an equivalent one, with the only variation being the lid material, which was ULTEM plastic in the alternative model.

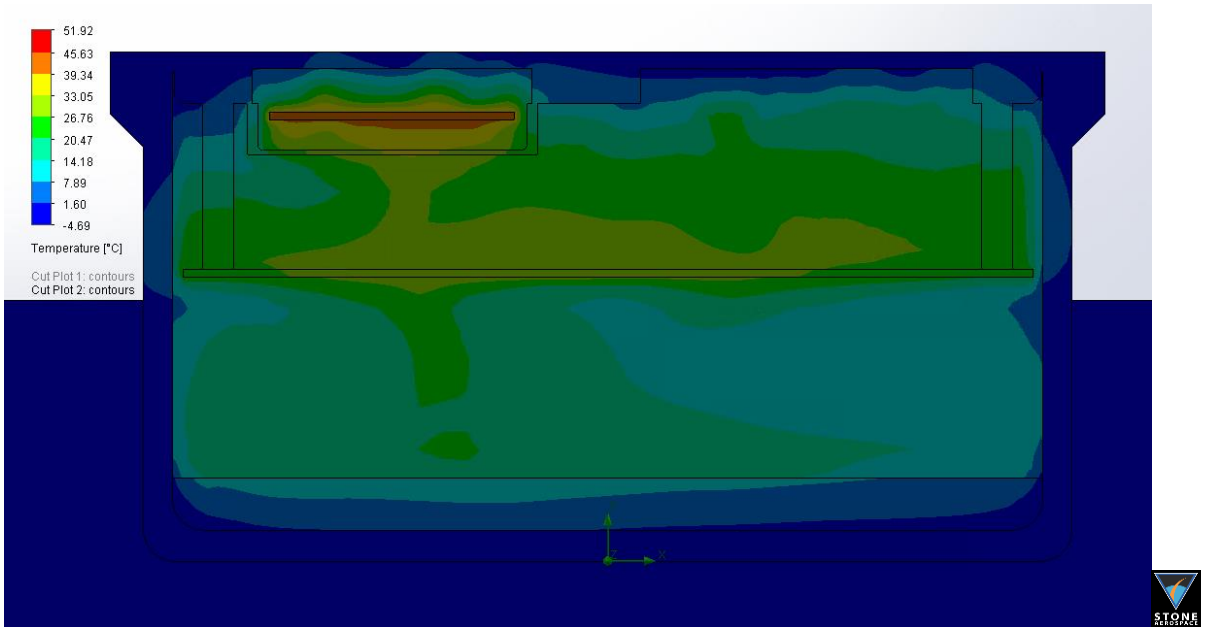

Figure 55: Puck thermal model comparison, employing an ULTEM lid and reaching up to 52°C, over 15 degrees above the aluminum lid model

These thermal model outcomes validate the chosen electronics arrangement and lid material. It's critical to recognize that these models serve to refine the design and should not be considered accurate representations of the actual temperatures within the puck. For true temperature measurements, tests in an environmental chamber at the University of Colorado are scheduled as future steps.

To tackle the challenge of achieving a threshold temperature prior to system startup, direct point heaters were recommended by the electronics team to elevate the boards to above-freezing temperatures before initiating power throughout the system. These heaters, delivering 9 W directly to the HackRF, Raspberry Pi, and FAM board, deactivate once the threshold temperature is attained, ensuring a safe operation of the system.

6 Conclusions

In this thesis, an in-depth exploration into the design and analysis of the PARTI pucks prototype was undertaken, with the aim of advancing RF communication technology for cryobot missions in Ocean World Exploration. The comprehensive study began with establishing the context and laying down the mission and prototype requirements. These foundational elements led to the development of a series of iterative design concepts and analyses that ensured the reliability and functionality of the prototype.

One significant lesson learned from this process was the complexity involved in prototype development. The importance of an iterative design process became evident as the project progressed. This allowed for a delicate balance to be struck between over-engineering and functionality, which is critical for the efficient performance of the prototype in field conditions. Additionally, the selection of materials and understanding their limitations proved instrumental in overcoming design constraints. The usage of commercially available components and material trade-offs played a vital role in the decision-making process and ensured the feasibility of the prototype.

Addressing potential challenges, especially those related to field deployment, was a central aspect of this study. The thesis showcases how predicting and mitigating these challenges through careful design and planning is crucial. Moreover, the importance of guideline documentation for field operators was highlighted, as this documentation serves as a roadmap to ensure the efficient handling and deployment of the prototype in the field.

Furthermore, this work sheds light on the significance of the prototype in the realm of glacial studies. The PARTI pucks prototype represents a noteworthy advancement in communication technology for remote and harsh environments. Its design, characterized by careful material selection and an understanding of environmental challenges, serves as a clear demonstration to the value of the prototype in collecting and transmitting data in glacier environments.

The thesis also serves as a valuable case study in mechanical design. Through a real-world challenge and problem-solving approach in prototype development, a foundation for future research and development in similar technologies was established. The structural and thermal analyses performed were pivotal in

evaluating the design's efficacy and reliability under varying environmental conditions.

In conclusion, the PARTI pucks prototype, developed through a meticulous and iterative design and analysis process, stands as a significant contribution to the field of communication technology in remote environments. Through lessons learned, addressing potential challenges, and understanding the contributions to both communication technology and mechanical design, the objectives of this thesis are fulfilled. Valuable insights are provided, and the thesis serves as a reference for future projects. Moreover, it represents a tangible advancement in technology critical for Ocean World Exploration. The dedication to both the minute details and the broader vision has culminated in a prototype that promises to pave the way for further innovations in this exciting domain.

Bibliography

[1] Stone, W.C., Hogan, B., Siegel, V., Lelievre, S., and Flesher, C., “Progress towards an optically powered cryobot,” Annals of Glaciology, 55(66) 2014, DOI: 10.3189/2014AoG65A200.

[2] Stone, W., Bramall, N., Bywaters, K., Christner, B., Doran, P., Nadeau, J., Skidmore, M., THOR: Thermal High-voltage Ocean-penetrator Research platform, NASA Grant 80NSSC18K1738, 2018-2020, Report No. 2019-THOR-X01, October 31, 2019.

[3] Stone Aerospace, https://stoneaerospace.com/ (accessed Jun. 01, 2023).

[4] B. Dunbar, “Technology readiness level,” NASA, https://www.nasa.gov/directorates/heo/scan/engineering/technology/technology_readiness_level (accessed May 05, 2023).

[5] Zimmerman, W., et al., "Advanced Mini-Radio Wave Ice Tranceivers for Planetary/Small Body Inner Ice Communications", NRA 99-0SS-05, NASA Advanced Cross Enterprise Technology Development for NASA Missions, February 2000.

[6] Bryant, S. "Ice-embedded transceivers for Europa cryobot communications," Aerospace Conference Proceedings. IEEE, vol.1 (2002).

[7] Cwik, T., Zimmerman, W., Gray, A., Nesmith, B., Casillas, R. P., Muller, J., ... & Sengupta, A. (2018). A Technology Architecture for Accessing the Oceans of Icy Worlds.

[8] Pradhan, O., S. Sandeep, A. J. Gasiewski and W. Stone, "Design of a forward looking synthetic aperture radar for an autonomous cryobot for subsurface exploration of europa," 2017 IEEE International Geoscience and Remote Sensing Symposium (IGARSS) , Fort Worth, TX, 2017, pp. 1012-1015, DOI: 10.1109/IGARSS.2017.8127126.

[9] Stone, W.C., et al. 2011. Design and deployment of a four-degrees-of-freedom hovering autonomous underwater vehicle for sub-ice exploration and mapping.

Proceedings of the Institute of Mechanical Engineers, Part M: Journal of Engineering in the Maritime Environment. 224: 341061

[10] Stone, W.C., et al, "Sub-Ice Autonomous Underwater Vehicle Architectures for Ocean World Exploration and Life Search", in: Badescu V., and Zacny, K. eds, Outer Solar System: Prospective Energy and Material Resources, Springer, 2018, pp. 429-541. DOI: https://doi.org/10.1007/978-3-319- 73845-1

[11] Smeets, C., Boot, W., Hubbard, A., Pettersson, R., Wilhelms, F., Van Den Broeke, M., & Van De Wal, R. (2012). A wireless subglacial probe for deep ice applications. *Journal of Glaciology, 58*(211), 841-848. doi:10.3189/2012JoG11J130

[12] K. Martinez, R. Ong and J. Hart, "Glacsweb: a sensor network for hostile environments," 2004 First Annual IEEE Communications Society Conference on Sensor and Ad Hoc Communications and Networks, 2004. IEEE SECON 2004., Santa Clara, CA, USA, 2004, pp. 81-87, doi: 10.1109/SAHCN.2004.1381905.

[13] Prior-Jones, M., Bagshaw, E., Lees, J., Clare, L., Burrow, S., Werder, M., … Hubbard, B. (2021). Cryoegg: Development and field trials of a wireless subglacial probe for deep, fast-moving ice. *Journal of Glaciology, 67*(264), 627-640. doi:10.1017/jog.2021.16

[14] Guagliano, M. (2022). "Design for assembly (DfA) – 2. Joining methods for plastic parts." 054834 Methods for Advanced Mechanical Design, Politecnico di Milano, Milan, Italy. Lecture slides.

A. Appendix A: EMI Shield Snap-Fit Design

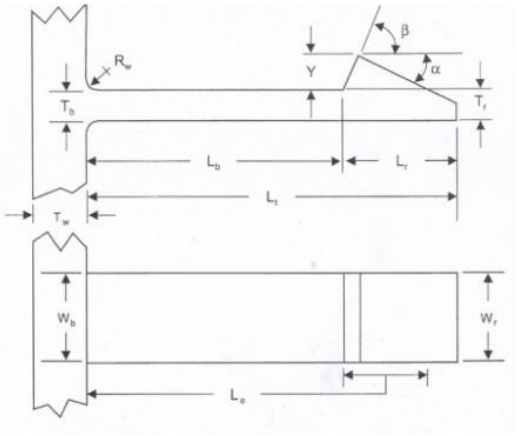

Figure 56: Snap fit design dimensions defining the joint [12]

$$Y = \frac{PL^3}{3EI} = \frac{4P}{Eb}\left(\frac{L}{t}\right)^3$$

Y = the deflection at the free end of the beam.

E=Elastic modulus

I=Moment of inertia=$\frac{1}{12}bt^3$

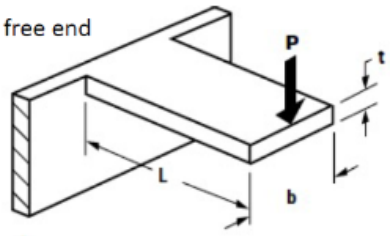

$$\sigma_{max} = \frac{PL}{I}\cdot\frac{t}{2} = \frac{6PL}{bt^2}$$

(nominal maximum stress and strain)

$$\varepsilon_{max} = \frac{\sigma_{max}}{E} = \frac{6PL}{Ebt^2} = 1.5\left(\frac{t}{L^2}\right)Y$$

Figure 57: Snap fit design, analytical formulas for a uniform cross-section based on the cantilever beam [12]

The notch effect must be considered.

$$K_t = \frac{\sigma_{max}}{\sigma_{nom}} = \frac{\varepsilon_{max}}{\varepsilon_{nom}}$$

(in many cases ≃1.5)

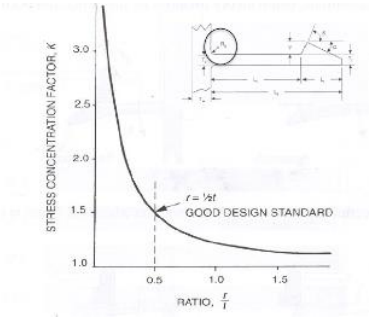

Figure 58: Snap fit design , notch effect [12]

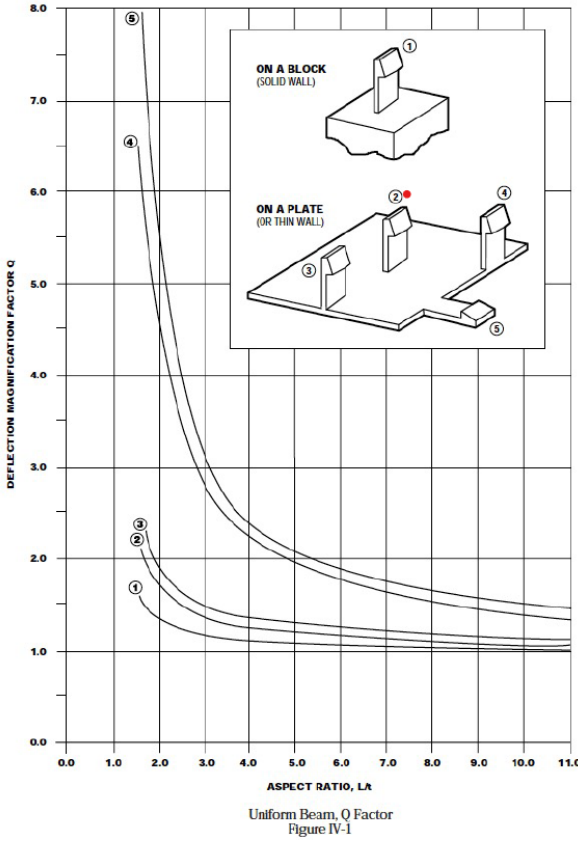

Figure 59: Snap fit design, corrective factor Q [12]

Table 11: Cell color coding for EMI box snap-fit calculations tables

Input
Intermediate
Output
Key Output

Table 12: Engineering calculations for the design of the UHF EMI box snap-fit, version A

UHF Box - version A						
		Metric Units		English Units		
Variable	Symbol	Value	Unit	Value	Unit	Data and recommended values
Material Properties						
Material		Nylon PA12				
Elastic Modulus, E	E	1750	MPa	253816.0	psi	1.7-1.8GPa
Ultimate Tensile Strength	UTS	48	MPa	6961.8	psi	
Elongation at break	ε	15	%	15	%	15-20%
Geometrical Data						
Tab thickness	Tb	0.940	mm	0.037	in	Key input
Beam length	Lb	8.89	mm	0.35	in	
Catch length	Lr	1.78	mm	0.07	in	
Total length	Lt	10.67	mm	0.42	in	
Force application length	Lo	9.78	mm	0.39	in	
Insertion angle	α	25	deg	25	deg	25-30deg
Insertion angle in radians	α	0.44	rad	0.44	rad	
Separation angle	β	40	deg	40	deg	Medium external separation loads
Separation angle in radians	β	0.70	rad	0.70	rad	
Tab radius	r	0.64	mm	0.025	in	
Wall thickness	tw	2.54	mm	0.1	in	
Overhang depth	y	0.60	mm	0.0235	in	
Width	Wr	4.70	mm	0.185	in	
Design checks: common design ratios						
Lb/Tb		**9.46**	-	**9.46**	-	At least 5, preferably 10
Lt/tw		**4.20**	-	**4.20**	-	
Tb/tw		**37.00**		**37.00**		50-60%

y/Tb		**0.64**		**0.64**		If Lb/Tb~5 <1 If Lb/Tb~10 =1
Deflection magnification factor	Q	**1.25**	Table	**1.25**	Table	
r/t		**0.68**	-	**0.68**	-	Target: 0.5
Stress concentration factor	Kt	**1.45**	Table	**1.45**	Table	

Stress and strain: permissible						
Permissible strain %	% allowed	0.20	-	0.20	-	
Max permissible strain	ε, perm	3.00	%	3.00	%	
Permissible deflection	y, perm	1.69	mm	0.07	in	

Stress and strain: actual						
strain, max	ε, max	**1.06**	%	**1.06**	%	
strain, eff	ε, eff	**1.23**	%	**1.23**	%	Lower than strain permissible
stress, actual	σ, actual	**21.5**	MPa	**3119**	psi	

Forces						
Cantilever force	P	1.52	N	0.342	lbf	

Insertion and separation forces						
Friction coefficient		0.40	-	0.40	-	Approximate
Insertion force per finger		1.48	N	0.33	lbf	
Separation force per finger		2.53	N	0.57	lbf	
Number of fingers		20.00	-	20.00	-	
Total insertion force		**29.61**	N	**6.66**	lbf	Target < 40 N
Total separation force		**50.60**	N	**11.37**	lbf	Target 40-50 N

Table 13: Engineering calculations for the design of the HF EMI box snap-fit, version A

HF Box - version A						
		Metric Units		English Units		
Variable	**Symbol**	**Value**	**Unit**	**Value**	**Unit**	**Data and recommended values**
Material Properties						
Material		Nylon PA12				
Elastic Modulus, E	E	1750	MPa	253816.0	psi	1.7-1.8GPa
Ultimate Tensile Strength	UTS	48	MPa	6961.8	psi	
Elongation at break	ε	15	%	15	%	15-20%
Geometrical Data						
Tab thickness	Tb	0.813	mm	0.032	in	Key input
Beam length	Lb	8.89	mm	0.35	in	
Catch length	Lr	1.78	mm	0.07	in	
Total length	Lt	10.67	mm	0.42	in	
Force application length	Lo	9.78	mm	0.39	in	
Insertion angle	α	25	deg	25	deg	25-30deg
Insertion angle in radians	α	0.44	rad	0.44	rad	
Separation angle	β	40	deg	40	deg	Medium external separation loads
Separation angle in radians	β	0.70	rad	0.70	rad	
Tab radius	r	0.64	mm	0.025	in	
Wall thickness	tw	2.54	mm	0.1	in	
Overhang depth	y	0.60	mm	0.0235	in	
Width	Wr	4.70	mm	0.185	in	
Design checks: common design ratios						
Lb/Tb		**10.94**	-	**10.94**	-	At least 5, preferably 10
Lt/tw		**4.20**	-	**4.20**	-	
Tb/tw		**32.00**		**32.00**		50-60%

y/Tb		**0.73**		**0.73**		If Lb/Tb~5 <1 If Lb/Tb~10 =1
Deflection magnification factor	Q	**1.25**	Table	**1.25**	Table	
r/t		**0.78**	-	**0.78**	-	Target: 0.5
Stress concentration factor	Kt	**1.40**	Table	**1.40**	Table	

Stress and strain: permissible						
Permissible strain %	% allowed	0.20	-	0.20	-	
Max permissible strain	ε, perm	3.00	%	3.00	%	
Permissible deflection	y, perm	1.95	mm	0.08	in	

Stress and strain: actual						
strain, max	ε, max	**0.92**	%	**0.92**	%	
strain, eff	ε, eff	**1.03**	%	**1.03**	%	Lower than strain permissible
stress, actual	σ, actual	**18.0**	MPa	**2605**	psi	

Forces						
Cantilever force	P	0.95	N	0.214	lbf	

Insertion and separation forces						
Friction coefficient		0.40	-	0.40	-	Approximate
Insertion force per finger		0.92	N	0.92	lbf	
Separation force per finger		1.58	N	0.36	lbf	
Number of fingers		32	-	32	-	
Total insertion force		**29.59**	N	**6.65**	lbf	Target < 40 N
Total separation force		**50.56**	N	**11.37**	lbf	Target 40-50 N

Table 14: UHF EMI box snap-fit summary calculations, showing only the input and output changes for version B of the prototypes

UHF Box - version B						
		Metric Units		English Units		
Variable	**Symbol**	**Value**	**Unit**	**Value**	**Unit**	**Comments**
Geometrical Data						
Thickness increase		8	%	8	%	
Tab thickness	Tb	1.015	mm	0.040	in	
Insertion and separation forces						
Total insertion force		**37.30**	N	**8.39**	lbf	+25% from version-A
Total separation force		**63.74**	N	**14.33**	lbf	+25% from version-A

Table 15: HF EMI box snap-fit summary calculations, showing only the input and output changes for version B of the prototypes

HF Box - version B						
		Metric Units		English Units		
Variable	**Symbol**	**Value**	**Unit**	**Value**	**Unit**	**Comments**
Geometrical Data						
Thickness increase		8	%	8	%	
Tab thickness	Tb	0.878	mm	0.035	in	
Insertion and separation forces						
Total insertion force		**37.28**	N	**8.38**	lbf	+25% from version-A
Total separation force		**63.70**	N	**14.32**	lbf	+25% from version-A

B. Appendix B: Thermal Analysis Setup

Table 16: Puck thermal analysis, computational domain and fluid subdomains

COMPUTATIONAL DOMAIN SIZE
X min: -0.303 m
X max: 0.303 m
Y min: -0.160 m
Y max: 0.157 m
Z min: -0.303 m
Z max: 0.303 m
X size: 0.606 m
Y size: 0.317 m
Z size: 0.606 m
FLUID SUBDOMAINS
Default fluid type: Gas/Steam/Real Gas
Fluids
Air
Coordinate system: Global Coordinate System
Reference axis: X
Thermodynamic Parameters
Static Pressure: 101325.00 Pa
Pressure potential: Off
Temperature: -5.00 °C
Flow parameters
Velocity in X direction: 0 m/s
Velocity in Y direction: 0 m/s
Velocity in Z direction: 0 m/s
Turbulence parameters type: Turbulence intensity and length
Intensity: 2.00 %
Length: 4.800e-04 m
Flow type: Laminar and Turbulent
Humidity: Off

Table 17: Puck thermal analysis, material properties

Material	Density [kg/m^3]	Specific Heat [J/(kg*K)]	Conductivity Type	Melting Temperature [K]	Thermal Conductivity isotropic [W/(m*K)]	Thermal Conductivity transverse [W/(m*K)]	Thermal Conductivity in-plane [W/(m*K)]
Ice	921.3	T dependent	Isotropic	273.15	T dependent	-	-
ULTEM 1010	1270	2000	Isotropic	-	0.22	-	-
Polyurethane foam	1075	1400	Isotropic	-	0.03	-	-
Brass	8390	0.38	Isotropic	-	123	-	-
Aluminum 6061	2688.9	T dependent, ~875	Isotropic	933.4	T dependent ~237	-	-
PCB-4 layers	2145	1136	Axisymmetrical / Biaxial	1000	-	0.25	16.5

Table 18: Puck thermal analysis, ice temperature-dependent properties

Ice		
T [C]	Specific Heat [J/(kg*K)]	Thermal Conductivity [W/(m*K)]
-3	2045.3	2.252
-10	1997	2.326
-20	1928	2.437
-40	1790	2.68

Table 19: Puck thermal analysis, physical features, mesh and initial conditions

MESH
Global Mesh Settings
Automatic initial mesh: On
Result resolution level: 5
Advanced narrow channel refinement: Off

Geometry Resolution

Evaluation of minimum gap size: Automatic

Evaluation of minimum wall thickness: Automatic

PHYSICAL FEATURES

Heat conduction in solids: On

Heat conduction in solids only: Off

Radiation: Off

Radiation in gases: Off

Time dependent: On

Gravitational effects: On

Rotation: Off

Flow type: Laminar and turbulent

High Mach number flow: Off

Humidity: Off

Free surface: Off

Default roughness: 0 micrometer

INITIAL CONDITIONS

Thermodynamic parameters

Static Pressure: 101325.00 Pa

Temperature: -5 C

Velocity parameters

Velocity vector

Velocity in X direction: 0 m/s

Velocity in Y direction: 0 m/s

Velocity in Z direction: 0 m/s

Solid parameters

Default material: Aluminum Nitride

Initial solid temperature: -5 C

Turbulence parameters

Turbulence intensity and length

Intensity: 2.00 %

Length: 4.800e-04 m

Table 20: Puck thermal analysis, boundary conditions

BOUNDARY CONDITIONS
Label: **BC-ice**
Description: Ice far away from puck is adiabatic and at a defined wall temperature
Outer Wall 1
Type: Outer Wall
Faces: COMPLETE THERMAL MODEL, PARTI PUCK ICE-1/Revolve1//Face, COMPLETE THERMAL MODEL, PARTI PUCK ICE-1/Revolve1//Face
Coordinate system: Global Coordinate System
Reference axis: X
Heat transfer coefficient: 0 W/m^2/K
Temperature of external fluid: -5 C
Label: BC-air
Description: All external surfaces except for ice section are in contact with cold air, with a heat transfer coefficient of 25 W/m^2/K at a defined temperature
Outer Wall 2
Type: Outer Wall
Coordinate system: Global Coordinate System
Reference axis: X
Heat transfer coefficient: 25.000 W/m^2/K
Temperature of external fluid: -5 c

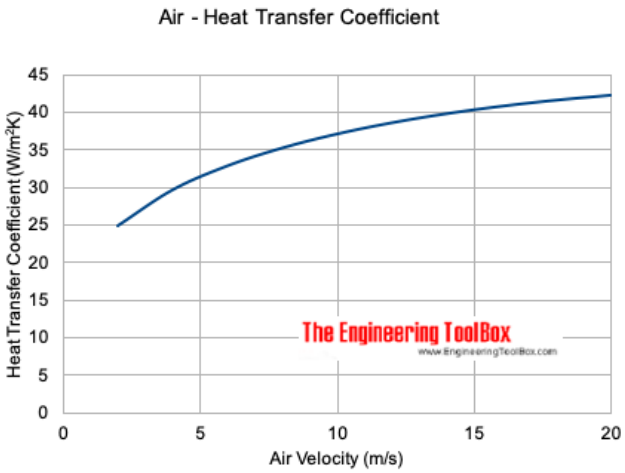

Table 21: Puck thermal analysis, heat sources

HEAT SOURCES
Label: HackRF
Heat Surface Sources
Components: HACK RF
Coordinate system: Global Coordinate System
Reference axis: X
Source type: Heat Generation Rate
Heat generation rate: 2.670 W
Label: Raspberry Pi
Heat Surface Sources
Components: RASPBERRY PI
Coordinate system: Global Coordinate System
Reference axis: X
Source type: Heat Generation Rate
Heat generation rate: 2.670 W
Label: Interface Board
Heat Surface Sources
Components: INTERFACE BOARD
Coordinate system: Global Coordinate System
Reference axis: X
Source type: Heat Generation Rate

Heat generation rate: 3.140 W

Label: HF Board

Heat Surface Sources

Type: Heat generation rate

Component: FAM BOARD

Coordinate system: Face Coordinate System

Reference axis: X

Toggle: On

Heat generation rate: 2.540 W

Label: UHF Board

Heat Surface Sources

Type: Heat generation rate

Component: FAM BOARD

Coordinate system: Face Coordinate System

Reference axis: X

Toggle: On

Heat generation rate: 2.860 W

I. List of Figures

Figure 1: Concept of a Cryobot with an RF communications puck deployed for Ocean World exploration. 3

Figure 2: NASA's Technology Readiness Levels [4] 4

Figure 3: In-ice testing of the UHF and HF antenna puck designs can be accomplished by using a moulin as a natural ice well 5

Figure 4: Glacsweb probe, with electronics and sensors housed in a 68 mm diameter plastic egg-shape capsule made of two halves permanently bonded [12] 7

Figure 5: Cryoegg probe, made of two halves of machined acetal copolymer sealed with an O-ring and eight machined screws [13] 7

Figure 6: FOXX Moulin profile map shows the feature has been mapped to over 100 m depth (left). A researcher investigates FOXX Moulin in 2019 (right, photo credit J. Gulley) 13

Figure 7: Preliminary design of the prototype pucks. Initially involving two separate puck designs: one for the patch antenna (top left) and another for the crossed-loop antenna (top right), and later on transitioning to a unified prototype puck (bottom) 15

Figure 8: UHF Patch Antenna Design....16

Figure 9: UHF Patch Antenna assembled on the bottom side of the puck housing 17

Figure 10: Rendering of the HF Crossed-Loop Antenna subassembly on the left, and picture of the subassembly attached to the puck lid through the five supporting standoff clamps, maintaining a one-inch distance from all other components 18

Figure 11: View from the top of the puck, looking at the User Interface on the lid.....19

Figure 12: Multiple views of the preliminary design of the prototype puck 20

Figure 13: Diagram of the prototype puck showing the four main sections of the design in different colors 21

Figure 14: Pie chart of the total part count in a puck per component category 22

Figure 15: Pie chart of the part count of mechanical components in a puck per category 22

Figure 16: View of the top and bottom surfaces of the Lid and Electronics Assembly with component labels 23

Figure 17: Exploded view of the FAM Board assembly with component labels 24

Figure 18: Exploded view of the Crossed-Loop Antenna assembly with component labels 24

Figure 19: Exploded view of the Housing and Patch Antenna subassembly with component labels 25

Figure 20: Top view of the Housing and Patch Antenna assembly, showcasing the SMA cables neatly coiled inside the insulation foam 26

Figure 21: Exploded view of the puck assembly, showing the custom mechanical components in purple 27

Figure 22: Color-coded transparent view of the puck highlighting different fastener materials utilized 31

Figure 23: Disassembly for Serviceability instructions manual for Operation A, opening the puck to separate Housing and Lid assemblies 32

Figure 24: Disassembly for Serviceability instructions manual for Operation B, separating the FAM and Crossed-Loop assemblies from the Lid assembly 33

Figure 25: Disassembly for Serviceability instructions manual for Operation C, separating the Crossed-Loop Antenna from the FAM Board.....33

Figure 26: Picture of the Bench Jig assembly in use.....34

Figure 27: Diagram of the different possible uses of the Bench Jig assembly for puck serviceability 34

Figure 28: Progressive design changes of the O-ring seal between the lid and the housing Components: lid in grey, housing in orange and O-ring in black 38

Figure 29: Picture of the three 3D printed housing variations for submersion tests, with different O-ring surface variations.....38

Figure 30: HackRF One EMI Shield. On the left, picture of the shield assembled to the lid. On the right, section view of the model, showing the tabs making contact with the lid and the EMI gasket shown in blue 40

Figure 31: HF and UHF circuits EMI Shields. On the left, picture of the shields to be installed on the FAM board. On the right, section view of the UHF model, showing the tabs, the snap fit groove on the brass base and the EMI gasket shown in blue 41

Figure 32: Progressive design changes of the User Interface components and locations on the prototype puck lid 41

Figure 33: Comparison of the electronic boards and user interface component locations. The final design arrangement has an increased available footprint for the interface board on the top left and presents a more symmetric design 43

Figure 34: Puck User Interface diagram with labeled features 44

Figure 35: Pie chart of the hardware cost breakdown for a prototype puck, color-coded in different shades by categories: mechanical components in orange, electronics components in green, and RF antennas in blue 46

Figure 36: Puck to ice test, using a puck-analog in an icy environment, to test rigging procedures 48

Figure 37: ULTEM 1010 mechanical properties, as reported by Stratasys 49

Figure 38: Housing finite element analysis constraints and loading conditions 50

Figure 39: Housing finite element analysis mesh 50

Figure 40: Housing finite element analysis, resulting stress and deflection plots of initial study, with a 34.3 N force applied 51

Figure 41: FAM Board finite element analysis assembly model 52

Figure 42: FAM Board structural analysis constraints, fixed surfaces shown in blue .53

Figure 43: FAM Board structural analysis loading, remote load applied on blue surfaces at the pink arrow location 53

Figure 44: FAM Board structural analysis mesh 53

Figure 45: FAM Board structural analysis deflection plots, normalized to .015 in (0.38 mm) and displaying 15 color gradients, so every color change represents a .001-in step 54

Figure 46: FAM Board connector location analysis, based on structural analysis deflection plots 55

Figure 47: Exploded view of the initial prototype puck design, with the electronic boards mounted to the FAM board 56

Figure 48: Puck preliminary thermal model results, performed on an assembly with electronics mounted on the FAM board 57

Figure 49: Puck Thermal Model Components 58

Figure 50: Puck thermal model, computational domain 59

Figure 51: Puck thermal model, main fluid subdomain in blue 59

Figure 52: Puck thermal model boundary conditions. BC-ice on the left, outer wall with no heat transfer, and -5°C. BC-air on the right, outer wall with 25 W/m^2K heat transfer coefficient at -5°C 59

Figure 53: Puck thermal model, mesh refinement level plot 60

Figure 54: Puck thermal model, temperature plot of the ZY (above) and XY (below) section views of the model 61

Figure 55: Puck thermal model comparison, employing an ULTEM lid and reaching up to 52°C, over 15 degrees above the aluminum lid model 62

Figure 56: Snap fit design dimensions defining the joint [12] 69

Figure 57: Snap fit design, analytical formulas for a uniform cross-section based on the cantilever beam [12] 69

Figure 58: Snap fit design , notch effect [12] 70

Figure 59: Snap fit design, corrective factor Q [12] 70

II. List of Tables

Table 1: Mission and Prototype Requirements 9

Table 2: Custom mechanical components by category, detailing manufacturing process, material and cost 28

Table 3: Color-coded exploded view of the puck highlighting different materials utilized 29

Table 4: Trade-off analysis of puck Housing manufacturing process 35

Table 5: Comparative matrix of commercially available 3D printing processes and materials. A red cell indicates a critical limitation, whereas a yellow cell denotes a point of concern 36

Table 6: Reference table of the User Interface indicator light labels and their meaning 44

Table 7: FAM Board structural analysis assembly components, materials and yield strengths 52

Table 8: Summary table of FAM Board structural analysis study results, given a load direction 54

Table 9: Puck Thermal Model components and materials 58

Table 10: Puck thermal model heat sources, as heat generation rates for each board component 60

Table 11: Cell color coding for EMI box snap-fit calculations tables 70

Table 12: Engineering calculations for the design of the UHF EMI box snap-fit, version A 71

Table 13: Engineering calculations for the design of the HF EMI box snap-fit, version A 73

Table 14: UHF EMI box snap-fit summary calculations, showing only the input and output changes for version B of the prototypes 75

Table 15: HF EMI box snap-fit summary calculations, showing only the input and output changes for version B of the prototypes 75

Table 16: Puck thermal analysis, computational domain and fluid subdomains 77

Table 17: Puck thermal analysis, material properties 78

Table 18: Puck thermal analysis, ice temperature-dependent properties 78

Table 19: Puck thermal analysis, physical features, mesh and initial conditions 78

Table 20: Puck thermal analysis, boundary conditions 80

Table 21: Puck thermal analysis, heat sources 81

III. List of Abbreviations

Abbreviation	Description
AUV	Autonomous Underwater Vehicle
CFD	Computational Fluid Dynamics
COLDTech	Concepts for Ocean worlds Life Detection Technology
COTS	Commercial Off-The-Shelf
CU	University of Colorado, co-investigator institution of the PARTI-Pucks project
EMI	Electromagnetic Interference
FAM	RF Feed, Amplification and Matching Network
FEA/FEM	Finite Element Analysis/Method
HF	High Frequency, between 3 and 30 MHz
NASA	National Aeronautics and Space Administration, an independent agency of the U.S. federal government
PARTI-Pucks	**P**uck-based data transmission using **A**daptive **R**adio modems for **T**hrough-**I**ce communications.
PEM	PEM® brand fasteners, with self-clinching technology
RF	Radio Frequency
SDR	Software Defined Radio
SMA	SubMiniature version A, coaxial RF connector
TRL	Technology Readiness Level
UHF	UltraHigh Frequency, between 300 MHz and 3 GHz

IV. List of Definitions

Term	Definition
Cryobot	Ice-penetrating vehicle
Disto-X	Device that measures distance, azimuth, and inclination used for surveying
Europa	One of Jupiter's moons, an ocean world beneath a thick layer of ice.
Moulin	Vertical, well-like shafts within glacier ice
Ocean World	Astronomical body with a current liquid ocean
PARTI-Pucks	Stone Aerospace project, in partnership with University of Colorado, funded by the NASA COLDTech program
Puck	Radio transceiver, commonly cylindrical in shape
Stone Aerospace	Texas-based aerospace engineering company dedicated to developing smart systems and tools needed to explore today's frontiers

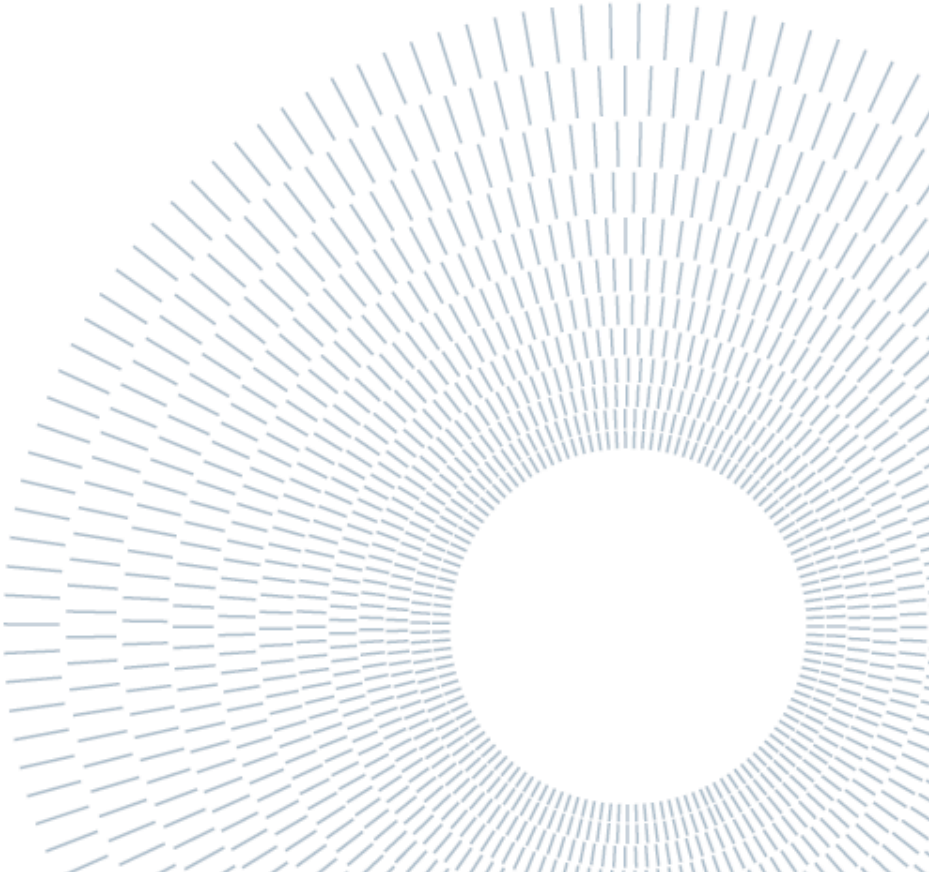

V. Acknowledgements

First and foremost, I am thankful to **Politecnico di Milano** for welcoming me and providing a platform to advance my career, through rigorous and high-quality education. I am thankful to all the **professors and faculty members** of the Mechanical Engineering Master's program. I am especially indebted to my thesis advisor, **Prof. Mario Guagliano**, whose guidance and support was essential to completion of this thesis. His course, Methods for Advanced Mechanical Design, was particularly influential and inspiring, both honing my skills and cultivating a deeper appreciation for the process of transforming a conceptual idea into a tangible prototype through iterative design. I am also thankful for all my **classmates** at Polimi who took part in this journey, which, for me, began in Austin, Texas. Starting the master's program during a global pandemic, and facing the added complexity of time zones, with exams as early as 2 am, was a big challenge, one that I overcame with the help of many supportive people.

I am deeply thankful to **Stone Aerospace**, the company that has allowed and encouraged me to grow from an undergraduate intern, back in the summer of 2018, to the engineer that I have become five years later. I appreciate all the opportunities for growth they have given me, including trainings, certifications and even preparing me to present at my first planetary science conference. I am especially grateful to **Dr. Bill Stone**, for his lead role in all the opportunities I have been given at the company, along with **Vickie Siegel** for their support and guidance in the process of writing this thesis and advancing meaningful technologies. I would also like to thank **Alberto Lopez**, for his mentoring role both professionally and academically, who, along with **Dr. Kristof Richmond**, advised me and fully supported my decision to start a master's program abroad while continuing my work at the company.

The PARTI-Pucks project was an especially rewarding one for me, in which I was able to apply the methodologies learned in the master's program, along with the skills developed with Stone Aerospace, from both an engineering and artistic perspective. This project has been a success due to all the incredible people involved. I would like to give special thanks to **Justin Smith**, the senior mechanical engineer of the project, for his excellent advice both in engineering and in life. I am thankful for

Kristi Erickson, who laid the groundwork for managing and achieving the project goals. And big thanks to the RF team, **Brian Pease** from Stone, and the CU team **Prof. Al Gaswevski** and **Jake Shali**, for their incredible talent in RF communication systems, which sometimes seems like black magic to me. I am deeply appreciative of the rest of the **Stone Aerospace team** who contributed in one way or another to the success of the project and this thesis.

A very special thanks goes to my **family and friends**, near and far, who supported me throughout this adventure and gave me the strength to keep going until the finish line. A **mis papás**, gracias por el apoyo incondicional en todas mis locuras e inventos y por inculcarme el valor de la educación. A mis **hermanas** y **abuelos** por todo el cariño, al igual que al resto de **mi familia y amigos** por chequear conmigo y preguntar si ya por fin pasé los exámenes. Por último, pero no menos importante, unas gracias inmensas a mi esposo **Gui** por estar conmigo a lo largo de todo este recorrido que parecía interminable. Las palabras no son suficientes para agradecerte por todo lo que me has apoyado, al igual que a **Cowboy** por siempre estar a mi lado en esas largas noches de estudio. A todos, de corazón, muchas gracias.

There are many other special people not listed here, including colleagues and friends, who were in some way a part of this journey. To them, I say thank you!